R. & M. No. 2902
(15,507)
A.R.C. Technical Report

MINISTRY OF SUPPLY

AERONAUTICAL RESEARCH COUNCIL
REPORTS AND MEMORANDA

Flight Tests at Transonic Speeds on Freely Falling Models

PARTS I to V

Edited by

C. KELL, A.M.I.Mech.E.

LONDON: HER MAJESTY'S STATIONERY OFFICE
1955
PRICE 8*s* 6*d* NET

Flight Tests at Transonic Speeds on Freely Falling Models

PARTS I to V

Edited by

C. KELL, A.M.I.Mech.E.

COMMUNICATED BY THE PRINCIPAL DIRECTOR OF SCIENTIFIC RESEARCH (AIR), MINISTRY OF SUPPLY

Reports and Memoranda No. 2902*

October, 1952

Summary.—In the past decade the problems associated with high-speed flight have increasingly occupied the minds of many workers in aerodynamics and aircraft structures. The possibility of achieving supersonic flight has introduced a number of new problems not the least of which has been that of obtaining aerodynamic information throughout the transonic range of speeds. This report deals with one of the early test techniques developed for this purpose.

Basic bodies carrying the aerofoils to be tested were released from an aircraft flying at height, and accelerated under the influence of gravity through the transonic speed range. Radar recorded the flight path and telemetering equipment carried within the body transmitted information to a ground station during the free fall.

The work on this method of test which was started in 1943 was brought to a close in 1949. The main reason for abandoning the experiments was the limiting accuracy of the telemetering equipment although other contributing causes were present.

Part I of this report is a historical precis of the work and Part II a description of the models and the technique itself. In Part III the drag measurements on nine wings are presented and in Part IV the application of the technique to flutter tests is considered. Part V discusses the accuracy of the technique.

PART I

Historical

by

C. KELL

Although it had long been recognised that as the speed of a body in a compressible fluid approached and exceeded the speed of propagation of a pressure wave there would be changes in the character of the flow associated with compressibility, this régime still remained, in 1939, the province of the research worker and the ballistician. The impetus given to aircraft design by the war, however, so accelerated progress that within a few years these compressibility problems attained practical importance. Although there was no detailed knowledge of what went on at sonic speeds, it was clear that the drag of the aircraft of that day rose rapidly; on the other hand there were indications that the ultimate development of the existing reciprocating

* R.A.E. Tech. Memo. Aero. 308.

engine-propeller power plant, in terms of thrust per square foot of frontal area, was being reached. Flight at sonic and greater speeds remained a goal not to be achieved by a straightforward development.

At this stage new methods of propulsion in the form of rockets, ramjets and turbo-jets gave promise of solving the thrust problem, and aroused intense interest in compressible aerodynamics. Experimental work had shown quite clearly that existing tunnels could not be made to yield useful data at Mach numbers between about 0·9 and 1·2. Supersonic aerodynamic theory was in its infancy, and theory for sonic speeds being virtually non-existent there was thus the need to develop new methods of research for the transonic region. It was apparent also that the most immediate need was for information on the behaviour of the drag of wings and bodies.

As suggested above, projectiles such as bullets, shells, rockets and bombs frequently travelled at supersonic speeds, and these came under review in relation to the present problem. In October 1943 McKinnon-Wood proposed that use be made of the freely falling model technique[1]. Some preliminary calculations showed that if a dense body of high fineness ratio fitted with a non-lifting wing was released at about $M = 0{\cdot}4$ from upwards of 30,000 feet, sonic velocity would be reached and exceeded over a significant portion of the trajectory. By tracking the model with kine-theodolites or radar the trajectory could be determined, and by the use of radio telemetering or recoverable recorders the deceleration of the model and the force between wing and body could be determined. Thus it appeared possible to determine all the quantities essential to the calculation of the drag of whatever wings were fitted to a basic low-drag body.

This report describes the development of the freely falling model technique of research at transonic speed, its application to the measurement of drag on 9 wings, and to a study of the flutter characteristics of 4 wings. The experimental work was done between December 1943 and December 1949, and has been reported previously in Refs. 2 to 6 ; the present report summarises these five references.

A basic body some $13\frac{1}{2}$-ft long and 8-in. diameter was used ; it was fitted with stabilizing fins and weighed about 1500 lb. To this body were attached the test wings and within the body were fitted the instruments to telemeter to a ground station those quantities which would allow the drag of the model to be determined.

A problem with this work was that of aiming the model from an altitude of 35,000 ft so that it landed a safe distance from the ground receiving and control station, but at the same time was not so far away at any moment during the fall that the telemetering receivers were unable to obtain a satisfactory signal. It was also necessary to determine the position of the model in space throughout its fall in order to establish the appropriate atmospheric conditions during the test, and to establish the form of the trajectory for subsequent analysis of the results. Both these problems were overcome by installing at the ground site SCR.584 radar tracking equipment together with a specially designed plotting table.

Flight work was begun in December 1944 using a *Mosquito* B Mk. XVI for parent aircraft. Unfortunately this *Mosquito* crashed a few weeks later with the loss of both the aircrew. A replacement was not immediately available, and a *Mosquito* PR Mk. IX had to be accepted ; unlike the B Mk. XVI this aircraft had no pressurised cabin and in consequence long flights at high altitudes were very arduous for the aircrew. Nevertheless the special bomb crutches and the experimental equipment were installed and three dummy models, *i.e.*, ones without wings and telemetering equipment, were released from this particular aircraft to develop the technique. The first two dummy models were released at Pawlett range in Somerset in July/August 1945. Pawlett range was closed down shortly afterwards and the work transferred to Odstone range in Berkshire, where the third dummy model was released in September of the same year. On this occasion icing-up of the bomb-slip caused a temporary ' hang-up ' and the model fell away some seconds late ; it landed outside the range and caused some minor damage to private

property. Following this incident it was decided to transfer the work to Orfordness range in Suffolk where the models could be dropped into the sea. During the lull caused by the transfer of the ground equipment to this new range the opportunity was taken to transfer the aircraft equipment to a pressurised B Mk. XVI which had by then become available.

By August 1946 three dummy models had been released at Orfordness for training purposes and to prove the ground equipment. During the following two months four further models were released. Of these latter, which carried two-channel telemetering equipment, one model was a basic body without wings and the other three had rectangular wings of biconvex section and thickness/chord ratios of 12 per cent, 8 per cent and 5 per cent respectively.

In 1946 the group which had been engaged on this freely falling model work was called upon to extend its activities to cover work on rocket test vehicles air-launched from a parent aircraft. Orfordness was unsuitable for this new work because of the shipping concentration in adjoining waters, and its proximity to populated areas. A search was made for a site which would fulfil the requirements of both experiments and one was eventually found at the Scilly Isles. This group of islands is located in the Atlantic some 28 miles W.S.W. of Lands End and the largest of the group, St. Mary's Island, was chosen as a site for the ground equipment. By mid-1947 the installation work was complete and improvements based on the lessons learned at the previous ranges were incorporated. G.C.I. (ground-controlled interception) radar equipment existing at this site was of great value in assisting the SCR. 584 operator to locate and hold his target (the parent aircraft). The method of tying together the time of operation of the various cameras and recording apparatus was greatly improved. Hereafter six-channel telemetering equipment was employed.

The first model was released at the Scilly Isles range in August 1947, and was followed by two more before the end of the year. Of these the first two were dummies to check the new ground station set-up and to train new members of the ground crew, while the third was a test model fitted with rectangular wings of biconvex section and six-channel telemetering equipment. During 1948 four further models for drag investigation were released; one was a basic body without wings but with six-channel telemetering equipment and three had rectangular wings of RAE 101 section, 5 per cent, 8 per cent and 12 per cent thickness/chord ratios respectively and six-channel telemetering equipment. A further development and extension of the free fall technique now followed the issue of a note by Smith[7] in which he suggested extending the technique to investigate the flutter characteristics of particular wing forms: in November 1948 a wingless body was released to check the construction and telemetering equipment of models which were to be used for these flutter investigations.

During the following year, 1949, a total of ten models was released; five for drag investigation, four for flutter tests and one to investigate a multi-channel switched telemetering system[8]. Three of the drag models were fitted with swept-back untapered wings of RAE 101 section and thickness/chord ratios, in the free-stream direction, of 9·2 per cent, 6·1 per cent and 3·8 per cent respectively and two models were basic wingless bodies.

The Scilly Isles range proved to be very satisfactory for the freely falling model work, mainly due to the many improvements in the ground equipment brought about by the experience gained at the earlier ranges. With these improvements in the ground equipment, particularly in the accuracy of the telemetering recording apparatus, it became more and more evident that the accuracy of the airborne telemetering equipment had to be greatly increased if a tolerably accurate result was to be achieved. At the beginning of the work it was sufficient to be able to measure to within ten per cent the drag of a particular wing at transonic speeds, but later a much higher order of accuracy became essential if the tests were to be of practical value. Other methods of measuring drag at transonic speeds were being developed, in particular the ground-launched rocket model technique in which aids such as radio-Doppler had been developed to supplement and, for certain duties, to replace the relatively lower accuracy telemetering equipment. It appeared that unless the telemetering equipment used in the freely falling model work could be improved to a far greater extent than seemed possible within a short period of

time, then this method would not be able to compete against the ground-launched method. Much was done in this direction during 1949 but ultimately it became clear that without a complete redesign of telemetering equipment, involving as it must a considerable period of development work when no aerodynamic information would be obtained, then a high enough accuracy would not be achieved. In other respects the present method showed up badly when compared with the ground-launched technique ; the models were more difficult to handle because of their weight and they took longer to build. There was also the ever present problem of aircraft serviceability which reflected on the rate at which tests could be made. In view of these difficulties and the progress made in the ground-launched model technique it was finally decided to abandon the freely falling model work which was brought to a close at the end of 1949.

In Part V of this Report an analysis is made of the accuracy to be obtained using the free-fall technique.

PART II

Equipment and Technique

by

C. KELL and J. SWAN, B.Sc.

1. *Introduction.*—In this section it is proposed to describe the equipment and technique used for the freely falling model work ; although the emphasis is placed on drag measurements it should be understood that most of the technique and equipment described apply equally well to the flutter work.

2. *Test Equipment.*—2.1. *Model Data.*—Fig. 1 shows the general arrangement of the drag models used throughout the tests. Two types of basic body were used and in future we shall refer to these as type ' A ' or type ' B ' bodies ; the type B body was also used for the flutter experiments (*see* Part IV and Fig. 14). In both cases the body was formed from two lengths of 8-in. outside diameter steel tube, each length insulated from the other so as to form the two halves of a dipole aerial for the telemetering transmitter. With the exception of a cut-out for the wings and a small compartment for instruments in the type B body the whole of the forward section was filled with lead ; the rear section contained the telemetering equipment. The nose of the model was of cast iron with a nose-curvature radius of 3 body diameters, *i.e.*, a tangent ogive 1·66 body diameters long, and a sheet metal cone of 8 deg included angle was fitted to the tail. The weight of the model depended to a considerable extent upon the type of body used and the material from which the wings were constructed ; the lightest winged model weighed 1371 lb and the heaviest 1848 lb (*see* Table 1).

In the type A bodies (two-channel telemetering) the two recording instruments were mounted inside an airtight box at the rear of the body. This box was maintained at pitot pressure by a tube leading from the nose of the model (*see* Fig. 1). Pitot-pressure readings were then obtained from the deflections of an evacuated capsule and longitudinal acceleration readings from the movement of a spring-mounted weight constrained so as to move only in the longitudinal direction. In these early type A models the wing was rigidly fixed in the body ; on the later type B models the wing was mounted on plate-type springs so as to allow fore-and-aft movement. The wing movement which, during the free fall, depended on the drag of the wing and the longitudinal acceleration of the model, was measured by an inductance pick-up incorporated in the telemetering system,

The stabilizing fins on the first, type A, models were of rectangular plan form 0·625-in. thick. The later type B bodies had fins of larger area, the leading edge was swept back and the thickness reduced to 0·160 in. in an attempt to reduce their drag. For the same reason the external suspension hook of the type A bodies was replaced in the later bodies by one lying flush with the surface.

In all cases the drag wing had a net area of 8·89 sq ft and was mounted on the body at zero incidence. The wings had no dihedral and the fins were mounted at 45 deg to the wing axes (Figs. 1 and 2) to facilitate loading onto the parent aircraft. In all except two cases the drag wings were manufactured from mahogany ; the two exceptions (of low t/c ratio) were machined from stainless steel to obtain the requisite strength. Further details of the wing dimensions are given in Table 1.

On a number of occasions wooden dummy models without wings were released, mainly to check radar functioning and to develop further the operational technique. They were much lighter that the telemetering models and consequently did not reach the same speed.

2.2. *Aircraft Data.*—For the early tests at Pawlett and Odstone, *Mosquito* PR Mk. IX LR.479 was used. Since a pressurised cabin was so desirable the equipment was later transferred to *Mosquito* B.XVI PF.543 which was used thereafter throughout the tests at Orfordness and the Scilly Isles. Later still a second *Mosquito* B.XVI PF.604 which was primarily employed on a somewhat similar type of experiment was modified to carry models and so formed a reserve for the first aircraft.

Difficulties experienced in the radar tracking of the mainly wooden aircraft were overcome by applying an aluminium spray finish which provided a metallic reflecting surface for radar tracking.

A tubular framework attached to the aircraft centre-section inside the bomb-bay supported the model on a bomb slip, the jaws of which protruded below the closed bomb doors. The model was thus slung external to the aircraft (Fig. 2), being steadied by fore-and-aft crutch pads in the normal manner.

An automatic observer was fitted in the aircraft to record the air speed, altitude and air temperature when the model was released. A separate electric supply was carried in the aircraft so that telemetering transmissions could be made from the model from a source of known constant voltage prior to release, without causing any drain on the batteries carried within the model.

A series of flights was made on both PF.543 and PF.604 to determine the errors in their altimeters and air speed indicators due to the position of the static vent. The aircraft thermometers were also calibrated to determine the error due to compressibility.

2.3. *Radar Equipment.*—In Ref. 9 a comprehensive description of the ground equipment at the Scilly Isles range, and the method of aircraft control, has been given, so that in this section the ground equipment and the methods of operation will only be dealt with briefly.

The SCR.584 radar tracking gear was standard U.S. Army gun-laying equipment and was used to track the aircraft prior to, and the model after, release. A small amount of modification was made to the standard equipment in order to record slant range and angles of azimuth and elevation. The range was displayed on a cathode-ray tube and the angles on engraved protractors fitted to the moving aerial system. Up to the time of leaving Orfordness range these readings were recorded by three 16-mm cameras driven synchronously by selsyns but later, at the Scilly Isles range, one camera only was used and the scales photographed through a suitable mirror system. The radar equipment was situated a little off the bombing run of the aircraft so that the aerial was never required to ' look ' vertically upwards. This was important since, for a target at the zenith, the automatic tracking equipment was unable to decide whether to drive the aerial clockwise or anti-clockwise and as a result lost such a target.

The SCR.584 radar equipment tracked automatically in azimuth and elevation but the range tracking was by manual control. Immediately after release of the model it was not possible to distinguish between the ' echoes ' received from the aircraft and the model, since they were so close together. About 6 seconds after release the echoes from the model and the aircraft separated (*see* Fig. 4) and it was important at this stage that the range tracking operator should concentrate on the former. If the separation was followed successfully this far the automatic follow in azimuth and elevation would then track the model in preference to the aircraft.

Ground-controlled interception (G.C.I.) radar equipment was also installed at the Scilly Isles. This being ' search ' equipment its radar beam was not so restricted as that of the SCR.584, and thus allowed the target (the parent aircraft) to be located much more easily and at greater ranges than would otherwise have been possible. This equipment could not track the target automatically but was used for providing such information as would allow the restricted beam of the SCR.584 equipment to be manually directed to locate and ' lock on ' to the target.

2.4. *Aircraft Control.*—The information supplied by the SCR.584 radar apparatus in the form of range, elevation and azimuth was used to operate a plotting table so arranged that a spot of light passing over a glass topped map table indicated the projection on the ground of the flight path of the aircraft being tracked. A controller, by watching the plotting table was able to maintain the aircraft on a predetermined circuit by giving the pilot instructions by radio. By this form of control it was possible to keep the aircraft within range of the radar and telemetering reception site, and also release the model accurately along a predetermined bombing line from above complete cloud cover. The controller was kept informed by a look-out of the position of shipping in the area so that he could arrange to drop the model only when the area was clear. On the actual bombing run of the aircraft the controller gave the pilot the necessary compass courses to steer and informed him when the aircraft was immediately above the predetermined release point.

2.5. *Telemetering.*—2.5.1. *Airborne Equipment.*—In this section we shall refer mainly to the six-channel telemetering equipment used in the type B bodies. Apart from the increased number of channels available this was an improved version of the earlier type. A similar type of six-channel telemetering set has already been described elsewhere by the Staff of Supersonic Division RAE[9] (1950) ; all three employ the same operating principles which, briefly, are as follows.

Instruments sensitive to changes in those quantities to be measured were fitted to the model and arranged to vary in turn the value of an inductance. This inductance formed part of the tuned circuit of an audio oscillator, so that the audio frequency of each of six oscillators depended on the values of the physical quantities being measured by six instruments. By a suitable choice of range over which each inductance worked it was possible to arrange each audio oscillator to cover only a chosen band or ' channel ' of audio frequencies and thus avoid any mutual interference between channels. These six audio frequencies were mixed and used to amplitude modulate a 40 Mc/s carrier wave which was transmitted to the ground receiving station.

Fig. 3 shows the six-channel transmitter ; the chassis was made to slide into the rear casing of the model and consisted of a number of compartments containing the R.F. unit and modulator, the rotary converter, the audio oscillators and the L.T. power supplies. Whilst the model was attached to the aircraft the electrical supply was taken from the aircraft *via* a pull-away plug and socket and after release a relay automatically switched in the internal power supply carried in the model.

2.5.2. *Ground Equipment.*—The telemetering ground receiving equipment was sited some 500 yards away from the main radar and control centre in order to reduce the chances of receiving interference signals from the radar transmitters. The carrier wave from the model

transmitter was demodulated and the six audio frequencies separated by suitable filter circuits ; each frequency was then converted into a voltage which was displayed on a dial. The relationship between the quantity being measured in the model and the audio frequency of the appropriate channel was determined before the test by calibration of the airborne telemetering set. The ground station recording equipment was calibrated by feeding known frequencies through each filter circuit and reading the dials. During the fall of the model the indicator dials were photographed by a F.24 camera taking exposures at intervals of 1·2 seconds and also by a Bell and Howell A4 ciné camera operating at 10 frames per second. In addition six-channel continuous trace recording equipment was used to give a qualitative record of the various quantities as they varied throughout the flight.

2.6. *Timing.*—Prior to the move to the Scilly Isles range, the method of time recording was to have each camera photograph a clock in addition to the instrument ; experience in the analysis of the results showed however, that this method was not sufficiently accurate. At the Scilly Isles range a crystal controlled oscillator was installed and a dividing circuit included which operated relays at intervals of 0·1 and 1·0 seconds. These relays flashed mercury vapour lamps in an automatic observer and these flashes were recorded on a continuously moving film. To the shutters of all the other recording cameras contacts were fitted which operated relays whenever the appropriate shutter was opened ; these relays flashed individual mercury vapour lamps in the automatic observer. In this way the time of operation of each camera was recorded and related to a common accurate timing system.

3. *Method of Determining Drag.*—The main requirement from these tests was to determine the variation with Mach number of the drag of a series of wing plan forms and sections. To obtain stable flight and to house the telemetering equipment it was, of course, necessary to attach these wings to a body. The technique thus involved measuring the drag of the body and wings combined, and the drag of the body alone ; wing drag was then determined by difference. This method assumes that body drag did not vary between models and of course debits the wing with the interference drag of the wing on the body and of the body on the wing, but in the present models these effects are believed to be small. Some check on the validity of this assumption was attempted in some models in which, as described above, the force between wing and body was measured.

Now drag coefficient is given by :

$$C_D = \frac{\text{Drag}}{\text{some convenient area} \times \text{static pressure} \times M^2\gamma/2}$$

and it can be shown, Smith & Thom[10] (1945), that the ratio Drag/Weight is given by an accelerometer provided it is directed along the line of flight.

The variables to be determined were longitudinal acceleration, static pressure and Mach number. The model weight and dimensions were measured before the test and the value of γ assumed constant at 1·4.

To determine the value of static pressure p it was necessary to know the height of the model at any time throughout its fall. This information was obtained by computation from the SCR.584 radar record. The static pressures were then estimated from meteorological data obtained by sounding balloons or, for the last few tests, by flying the parent aircraft over the test area immediately after release of the model and measuring temperatures and pressures over a range of heights, determined by radar.

From the SCR.584 results a position-time curve was determined which when differentiated gave a curve of velocity against time. This process could then be repeated to give a curve of longitudinal acceleration against time. Both of these were legitimate processes but the order

of accuracy was low in the case of the resulting velocity-time curve and even lower in the case of the acceleration-time curve. The inaccuracies of these processes showed themselves as scatter in the results obtained; the causes of these inaccuracies were the basic inaccuracies in the radar tracking equipment and are dealt with in more detail in Part V of this report. The use of kine-theodolite equipment would have greatly reduced these errors but weather conditions in this country are seldom good enough to use these instruments for this particular type of work. From radar then, sufficient information was available to determine height, from which the static pressure was deduced, and by differentiation usable values of velocity were obtained, which in conjunction with temperature at the appropriate height, allowed the Mach number to be determined.

Now longitudinal acceleration was obtained from the telemetered accelerometer reading by the relation:

Longitudinal acceleration $\div g$ = sine of model axis to horizontal — accelerometer reading (g units) Ref. 10.

The flight-path angle which was almost the same as the angle of the body to the horizontal was determined from the radar information, and the value of the longitudinal accelerometer reading was telemetered continuously throughout the fall. Knowing the weight of the model it was therefore possible to determine drag.

To these results there was a small correction to be made for the effect of wind speed and direction. The correction to velocity derived from radar was merely that of adding the component of wind along the axis of the model. Now the model always pointed in the direction of the relative airflow so that the angle of the model axis to the horizontal and the angle of the flight path to the horizontal were different when a wind was blowing. This difference had to be accounted for when using the flight-path angle to determine the longitudinal acceleration of the model.

The telemetered accelerometer information allowed a second approach to be made to the determination of velocity. The velocity of the parent aircraft at release was known from the air speed indicator, altimeter and thermometer readings and the integration of the longitudinal acceleration derived from telemetering was added to the release speed to give a curve of velocity against time. In Fig. 5a typical height-time and velocity-time curves are shown and in Fig. 5b typical Mach number-time and acceleration-time curves.

In all but the last three telemetered models total-head pressure was measured at the extreme nose and from this and estimates of static pressure already mentioned, another estimate of velocity could be made. Unfortunately, telemetering was such that a great enough accuracy could not be obtained to make this method of velocity determination worth while.

Arrangements were made in the models with six-channel telemetering to measure the static pressure by means of a series of holes drilled radially at the junction of the nose ogive and the parallel part of the body. These holes led to a common chamber which in turn was connected with a pressure sensitive pickup. Accuracy was disappointingly low and it was difficult to separate the errors due to telemetering and those due to the position of the measuring holes. In the last three models the static pressure was measured at a point 0·25 diameters ahead of the nose but in this case the results were influenced by the presence of the bow shock-wave. Further details of these measurements are given later.

In the flutter experiments (*see* Part IV) the use of the range was almost identical with that described above. The principal difference was that the telemetering equipment was now used to record, in addition, oscillations and failure of the wings due to flutter.

PART III

Drag Experiments

by

C. KELL and F. SMITH, M.A.

1. *Introduction.*—It has already been pointed out that the main difficulty with the work was in the analysis and interpretation of the telemetering results. In particular the presence of frequency drift in the telemetering results made their analysis very difficult and, as will be shown in Part V, even a small amount of drift could lead to a large error in the final result of drag coefficient. It would be tedious and of little practical value to take each test in turn and explain what errors were obviously present at the start of the analysis and what was done to reduce them. Generally speaking it may be said that telemetering results have been used where it has been possible to check telemetering at some point of its range against some other independent source of information. For example, the drag, and therefore the value the longitudinal accelerometer should indicate, could be estimated with reasonable accuracy for the moment of release. When integrated and added to the accurately known release speed, the longitudinal accelerometer results could be compared with the velocity derived from the radar position-time curve. If the estimated and measured values of acceleration at release agreed with one another and the velocities derived from differentiation and integration also agreed then the accelerometer readings could be used with confidence to determine drag.

For convenience we shall divide the results into three groups, *viz.*,

I Tests of rectangular wings of biconvex section.

II Tests of rectangular wings of RAE 101 section.

III Tests of swept-back untapered wings of RAE 101 section.

This is also the chronological order in which the tests were made.

2. *Tests on Rectangular Biconvex Section Wings* (Group I).—Details of the wing plan-form and other relevant data concerning these models are given in Table 1 under Group I models. Three wings were tested having 5 per cent, 8 per cent and 12 per cent thickness/chord ratios respectively. The bodies for these models were all type A, *i.e.*, they were fitted with rectangular stabilizing fins and two-channel telemetering equipment.

In Fig. 6a the overall drag coefficients of the models are shown plotted collectively; also included is the drag of the basic body alone. The results of the first model with 5 per cent thick wings were difficult to interpret and suggested that the wings broke off during flight. This was a possibility since the wings were rather weak but as the radar equipment failed to track the model during the latter part of the fall no confirmation could be obtained. A second model was therefore tested and the results given are for this model. Unfortunately on this second model an electrical fault developed and the telemetering failed to work. Consequently the results in this case were obtained from the double differentiation of the radar position-time curve; this accounts for the considerable scatter in the results for this model.

In an earlier part of this report it was mentioned that a number of wooden dummy wingless models were released. The radar results of one of these were analysed. Now the accuracy of analysis of the radar results depends on the ratio of the drag to the weight so that the larger the drag/weight ratio the more accurate the results. Since a dummy model only weighed about one fifth the weight of the telemetering models the accuracy was appreciably greater than that obtained by analysis of the radar tracking of the fully weighted models. The results from the dummy model analysed are shown plotted in Fig. 6a with those from a body fitted with telemetering. The agreement between the drag coefficients obtained from the dummy and the telemetered model is quite good.

The drag coefficients of the wings alone based on net wing area are shown in Fig. 6b. These results were obtained by subtracting the drag of the basic body from the drag of the model

with wings and relating the answers to the net wing area instead of body frontal area. The results therefore include the effect of interference drag.

In Fig. 6c the drag coefficients, based on net wing area, near $M = 1$ have been plotted against wing maximum thickness/chord ratio. The results suggest that at $M = 1$:

$$C_D \text{ (based on wing area)} = 0{\cdot}005 + 0{\cdot}72\left(\frac{\text{Thickness}}{\text{Chord}}\right).$$

The value 0·005 is an estimated figure for the skin-friction coefficient in this speed range*.

3. *Tests on Rectangular* RAE 101 *Section Wings* (Group II).—The models in this group all had type B bodies, *i.e.*, fin leading edge swept and six-channel telemetering. As for the previous models wings of 5 per cent, 8 per cent and 12 per cent thickness/chord ratios respectively were tested as well as the body alone. Details of the models are given in Table 1.

On the model with the 8 per cent thick wing telemetering failed completely on the channel containing the longitudinal accelerometer and the results quoted are for the double differentiation of the radar tracking. For the remaining channels of this model and for all channels of the other models the analysis showed there had been a drift in the telemetering which invalidated the original calibration curves. An estimate of the drift in the longitudinal accelerometer reading was made for the models with 5 per cent and 12 per cent wings by comparing the actual longitudinal accelerometer reading just after release with that predicted from the estimated low-speed drag of the model. For all other channel transmissions reasonable allowances of drift were made where the results looked promising but some results were not capable of interpretation, *e.g.*, the direct measurement of wing drag was possible only on the 5 per cent thick wing (*see* Fig. 7b). The effect of this drift on the accuracy of the results is discussed at length in Part V.

Fig. 7a shows the C_D vs Mach number relationship for the three Group II winged models and the wingless type B one.

Atmospheric temperature, pressure and wind speed corrections to these results were based on estimated values of these quantities obtained from the Air Ministry Meteorological Office.

At about the time that this group of tests was being made facilities were becoming available for tests using the ground-launched rocket model technique and the opportunity was taken to launch two wingless models similar to the basic wingless body used in the free fall tests. For reasons of manufacture the body diameter of the ground-launched models was reduced from the 8 in. of the free-fall body to $7\frac{1}{4}$ in. and all linear dimensions scaled down in the same proportion. The rocket outlet at the tail of the body necessitated a reduction in the length of the tail cone and an equivalent reduction in the total model length of 9·4 per cent. It is thought that this reduction in tail cone length resulted in no significant change in body drag. The velocity and acceleration of these models was determined from the analysis of reflection Doppler results and position-time data from Askania kine-theodolite equipment. Fig. 8b shows the C_D vs Mach number relationships of these two models. The agreement between the two results is so good that it can be accepted with confidence as the basic body drag of the free-fall models using type B bodies†. A comparison between the results of the free-fall models and the ground-launched models is given in Fig. 8c.

---

* This interpretation was the one which was placed on the results when they were first available (1947) ; since that time however, accumulated experience would suggest that in fact, for these wings, the relationship is much closer to $C_D = C_{Df} + K(t/c)^{5/3}$ where C_{Df} is skin-friction coefficient and K is a constant.

† It will be noted that in Fig. 8a, the free-fall models, there is practically no scatter in the results, whereas in Fig. 8b, the ground-launched models, a certain amount of scatter is present. It should be pointed out, however, that in the latter case the determination of each point is independent and unrelated to the other points, the maximum probable error being shown by the degree of scatter. In the former case each point is obtained by an integration process and is thus dependent on the accuracy of all the previous points ; it is therefore possible for errors to be present without these errors showing up as scatter.

The drag coefficient for the wings alone is shown plotted in Fig. 7b, as before these were obtained by subtracting body-alone drag from total body-plus-wing drag.

In the case of the 5 per cent thick wing a value for the wing drag alone, as given by the wing drag unit, is included. It must be remembered that the uncertainty in the result is high because of the unknown value of telemetering drift in this case, and no aerodynamic significance is attached to the difference between the two curves for the 5 per cent wing in Fig. 7b.

In Fig. 7c, C_D based on wing net plan area for values of Mach number near unity are plotted against (thickness/chord ratio)$^{5/3}$ (Kármán[11] (1942)).

4. *Tests on Swept-back Untapered* RAE 101 *Section Wings* (Group III).—The models in this group all had type B bodies ; the wings were untapered and were swept back 40 deg. The chord at right-angles to the leading edge was the same as for the other groups of wings, *i.e.*, 20 in. and the net wing area was again 8·89 sq ft. The only dimensional difference between the three models was the wing thickness/chord ratios which were 3·8 per cent, 6·1 per cent and 9·2 per cent respectively. These ratios refer to the chord along the free-stream direction. Taking the chord at right-angles to the leading edge these thickness ratios become 5 per cent, 8 per cent and 12 per cent respectively. In future the ratio in the free-stream direction will be quoted unless otherwise stated.

In Fig. 9a the total-drag coefficients of the three winged models are shown plotted against Mach number ; in all cases the results were obtained from telemetering gear after corrections had been applied for the effect of frequency drift. In all cases good agreement was obtained between the velocity obtained by integrating the acceleration and that obtained by the differentiation of the radar tracking.

For the models with 9·2 per cent and 6·1 per cent wings the atmospheric temperature, pressure and wind speed corrections to the results were based on measurements made over the dropping area by the parent aircraft immediately after the model was released. The results on the 3·8 per cent wing were based on figures predicted by the Air Ministry Meteorological Office. In Fig. 9a the C_D vs. Mach number relationships for a wingless model are also plotted. These results are those which were obtained by means of the ground-launched model technique and were dealt with in section 3 above.

The drag of the three wings shown in Fig. 9b has been obtained by subtracting the drag of the body alone from that of the appropriate winged model. For the 9·2 per cent and 6·1 per cent wings the wing drag alone, as obtained from the wing drag unit, is also shown plotted in Fig. 9b. In the case of the 6·1 per cent wing agreement with the total-drag minus body-drag is quite good considering the assumptions made in interpretating the telemetered information but for the 9·2 per cent wing agreement in the transonic and supersonic range is very poor ; in this range there is a considerable difference between the two wing drag unit results themselves. No direct wing-drag measurements were obtained on the 3·8 per cent wing because of a telemetering fault. It has already been pointed out that agreement between the velocity obtained by the integration of acceleration and that given by radar tracking was good. The total-drag minus body-drag which was obtained from the same accelerometers is therefore considered to be more reliable than that given by direct wing-drag measurements where no such comparisons can be made.

In Fig. 9c the experimental results of drag of the three swept-back wings above $M = 1 \cdot 1$ have been plotted against (thickness/chord ratio)^2. The results fall reasonably well on a straight line ; a skin-friction coefficient of 0·005 has been assumed.

In Fig. 10 a comparison is given of the drag of the three swept wings and the three unswept wings of the same wing net plan area and section dealt with in section 3.

A comparison has also been made and is shown in Fig. 11, of the experimental results obtained on the three swept-back wings and the theoretical drag suggested by Harmon[12] (1947). The theoretical results are based on thin symmetrical biconvex parabolic-arc sections whilst the

experimental results refer to RAE 101 sections with maximum thickness at 31 per cent of chord measured from the leading edge. For the theoretical analysis the thickness to chord ratio in the direction of the free stream has been used. In the case of the two thinner wings agreement is quite good ; it is not so good for the thick wing and the experimental results do not go to a high enough Mach number for any definite conclusions to be drawn. For the theoretical results an estimated skin-friction coefficient of 0·005 has been used.

5. *Static-Pressure Measurements.*—As a body passes through the transonic range a bow-wave, starting theoretically at infinity at $M = 1$, approaches the nose as the Mach number increases. The static pressure behind this shock is, of course, different from the free-stream pressure. Attempts to measure the free-stream pressure ahead of the nose of a given body will therefore lead to an error depending on the position of the static-pressure measuring holes in relation to the nose of the body, and the Mach number.

On the three bodies dealt with in section 4 above, a static-pressure tube was fitted to the nose of the body and led through the body to a static-pressure instrument with a pick-up on one channel of the telemetering system. This tube which was $\frac{1}{2}$ in. outside diameter and was closed at the forward end, protruded 7 in. from the front of the ogival nose. Slots were cut in the walls of the tube 5 in. back from the leading edge of the tube.

Estimates have been made by two methods given by Moeckel[13] (1949) to determine the Mach number at which the detached nose shock-wave passed over the static holes ; the result of these estimates is shown in Fig. 12. In Fig. 13 the difference between the recorded static pressure and the estimated free-stream static pressure has been plotted in non-dimensional form against Mach number. Agreement between the results for the three models is fairly good above $M = 0·9$; below this value the pressure difference and value of dynamic pressure become so small that small errors in the measurement of static pressure leads to large errors in the non-dimensional pressure difference. It would be expected that the change in pressure after the bow-wave had passed over the static holes would be more sharply defined than the experimental points indicate but it is probable that the lag in the pressure-recording instrument would account for this discrepancy.

In Fig. 13 the theoretical pressure rise through the shock-wave is also plotted and the values marked off at the Mach numbers corresponding to those at which the shock-wave is estimated, by the methods of Ref. 13 to pass over the static holes. It will be seen that on the three models tested the point where the pressure begins to fall off rapidly, *i.e.*, where the shock-wave passes, lies between the two values given by theory and the order of magnitude corresponds fairly well with theory.

PART IV

Flutter Experiments

by

W. G. Molyneux, B.Sc., and E. W. Chapple

1. *Introduction.*—The use of the freely falling model technique for flutter testing was first suggested by Smith[7] in 1948. The technique was attractive in that it offered a means of flutter testing in the transonic speed range where a wind tunnel cannot normally be used.

Much of the equipment used for steady-flow research was suitable for flutter, and in particular the ground equipment and telemetering transmitter were common to both. Additional items of equipment required were vibration pick-ups to measure the flutter oscillations and a mechanism to disturb the wing at intervals during the free fall to ensure that flutter was initiated when the flutter speed was reached. It was, of course, necessary to design wings with the flexibility required for flutter work.

Four flutter models in all were tested at the Scilly Isles range during the period March to October 1949, and the tests are described in detail in a report by Molyneux and Chapple[6] (1950). Flutter failures were obtained on two of the models and the remaining two failed under steady airloads. An attempt was made to obtain information on the drag of the models, but with little success due to drift and intermittent operation of the telemetering units.

2. *Details of a Complete Model.*—2.1. *Body of the Model.*—The bodies used for flutter work were similar in external appearance to the type 'B' body used for the steady aerodynamic tests (*cf.* Figs. 1 and 14) but their average weight was 500 lb. This weight was chosen so that a Mach number slightly greater than unity could be achieved during the fall from about 35,000 ft. Two types of body were used. In type B1 the wings were fixed directly to the body giving effectively fixed-root conditions, and in type B2 the wings were fitted to a model fuselage inside the shell of the body and attached to it by a drag link pivoted at one end to a bulkhead in the body and at the other to a point on the fuselage close to the centre of gravity of the wing-fuselage combination. The latter arrangement allowed the wing and fuselage to pitch relative to the body about two independent axes, which, for small amplitudes, can be regarded as representative of the freedoms in pitch and vertical translation on the model wing-fuselage combination. Practical considerations limited the amplitudes of the motions of the fuselage to $\pm$ 0·4-in. translation and $\pm$ 3-deg pitch. A complete model with the type B2 body is shown in Fig. 14.

2.2. *The Wings.*—Four wings in all were tested. Two of the wings had the same plan form as the untapered, 40-deg swept-back wings used for the steady aerodynamic tests (Group III). The wing chord normal to the leading edge was 20 in., the net wing area was 8·89 sq ft, the thickness/chord ratio was 7·7 per cent in the free-stream direction and the wing section was RAE 101. The wings were constructed of a light internal wooden structure of ribs and stringers to which a 3/64-in. thick plywood skin was attached. One was tested on a type B1 body and the other on a type B2 body, and by comparing the flutter results for the two wings it was thought that an indication of the effects of the body freedoms on wing flutter could be obtained.

The remaining two wings were scale models of a particular aircraft design and their flutter characteristics were required both to indicate the flutter characteristics of this design and as a check on flutter calculations. One wing was tested on a type B1 body and one on a type B2 body. The stiffness and inertia of the fuselage in the type B2 body were true to scale, and a scale representative tailplane was carried on a boom from the fuselage which protruded through a slot in the shell of the main body. This enabled the aerodynamic forces on the tail to be represented.

2.3. *Recording Instruments.*—Two types of instrument were used in each model. One recorded steady longitudinal accelerations in the range from $-$ 0·2g to $+$ 1·2g (the natural frequency of the instrument was 30 cycles/sec), and the other recorded oscillating forces normal to the wing plane in the range $\pm$ 10g (natural frequency 150 cycles/sec).

Various methods of damping the natural frequency of the instrument were attempted in the course of the tests, but the most successful method used was to immerse the movement in a light oil. However this reduced the sensitivity of the oscillation pick-up. The sensitivity was also changed by the effect of temperature on the viscosity of the oil.

For tests with the type B1 body one oscillation pick-up was fitted in each wing, and with the type B2 body there were pick-ups in each wing and also at the front and rear of the fuselage. A longitudinal accelerometer was carried in the body of all models.

2.4. *Flap Mechanism.*—Two mechanically operated flaps were used to create an intermittent turbulence over the wings to ensure that the critical flutter speed was not exceeded before flutter began. The mechanism was contained in a compartment in the nose of the main body (*see* Fig. 14). The flaps were operated by a motor-driven cam and were pushed out normal to the air stream at approximately half-second intervals during the fall.

3. *Test Procedure.*—The complete model was weighed and nose ballast was used to adjust the position of the centre of gravity so that the margin of pitching stability of the model in free fall was adequate. For tests with the type B2 body it was also necessary to ensure that the wing-fuselage combination itself had an adequate margin of pitching stability. This was achieved by using springs from the body to the nose of the fuselage. The springs served a further purpose in that they counteracted some of the inertia of the drag link under flutter conditions. All models were resonance tested, and the resonance frequencies and positions of the wing nodal lines were recorded. The longitudinal accelerometer was calibrated on its own telemetering unit and flight tests were made to check the equipment under high altitude conditions.

The models were released at the Scilly Isles range using the methods of aircraft control and data recording described in Part II.

4. *Discussion of Results.*—The telemetering units gave trouble on all models during the initial calibrations, and on three models they transmitted only intermittently during the fall. However the results obtained indicated that wing failures occurred on all four models. The 40-deg swept-back wings both appeared to fail due to flutter, but whereas the flutter of the wing on the type B1 body was ' flexure-torsion ' in character the character of the oscillations of the wing on the type B2 body was more compatible with a self-maintained oscillation caused by the fuselage striking the limit stops. This form of oscillation is generally referred to as backlash flutter. The records for these two wings are shown in Fig. 15. On the first record the action of the flaps in disturbing the wing can be seen clearly. The flaps did not operate on the second model and were probably frozen up. However, the wing oscillated for a considerable time and the frequency of the oscillations increased as the air speed increased, as would be expected from backlash flutter.

No oscillations prior to wing failure were obtained on the scale models, and the final failures were almost certainly due to the steady aerodynamic load resulting from a combination of change of trim with Mach number and bending moment due to wing ' wash-out '. If the wings had been constructed with symmetrical aerofoil sections, rather than with the cambered sections appropriate to the aircraft design, and with no wing washout, these failures could probably have been avoided. Provided the wing stiffnesses and inertias remained unchanged these modifications would not be expected to affect the classical flutter characteristics. The speeds at which the wings failed were in excess of the maximum design speed of the full-scale aircraft so that the tests established that wing flutter was not critical for the full-scale design. However, since no indications of flutter were obtained the tests provided no data to compare with flutter calculations.

The readings of the longitudinal accelerometers were unreliable on all the models due to drift and intermittent operation of the telemetering unit, so that the drag of the models could not be determined.

5. *Conclusions.*—Flutter oscillations were recorded on 40-deg swept-back wings under fixed-root and free-fuselage conditions. The fixed-root flutter was of the conventional flexure-torsion character but backlash flutter was obtained with the free-fuselage model due to the fuselage striking the limit stops. Tests on scale wings of a particular aircraft indicated freedom from flutter within the speed range of the full-scale design.

The general conclusion is that information on flutter at transonic speeds could be obtained by this technique. However the technique is laborious and considerable development, particularly of the telemetering unit, would be required before it could be considered reliable enough for general use.

6. *Further Developments.*—No further flutter tests using free-falling models are contemplated. Ground-launched rockets provide an alternative means for flutter tests at transonic speeds, and reliable results have been obtained by this method.

PART V

Notes on the Accuracy of the Freely Falling Model Experiment

by

T. F. C. LAWRENCE, B.Sc., B.E.

1. *Introduction.*—The work described in the present report concludes a programme of experiments, initiated at the end of 1943, which has provided drag curves on 9 wing shapes ; of these results it is considered only those in Group III are sufficiently reliable to be useful. The technique has now been abandoned and it seems appropriate to consider critically the method, in particular the accuracy and reliability of the answers it provides.

2. *General Statement of the Method.*—The answer to an experiment is presented, in Fig. 6b for example, as a curve of drag coefficient plotted against Mach number, where

$$C_D = \frac{D}{\frac{1}{2}\gamma p M^2 S},$$

$$M = \frac{V_a}{a},$$

and

C_D Drag coefficient

D = Drag (lb)

p Local absolute air pressure (lb/sq ft)

$= 2116{\cdot}2\,p'$
where p' is the local relative air pressure

M Mach number

V_a True velocity relative to air (ft/sec)

a Local velocity of sound (ft/sec)

$= 65{\cdot}9\sqrt{T}$
where T is the local absolute air temperature (deg K)

S Reference area (sq ft)
$\gamma = 1{\cdot}4$
} constants.

In this experiment, the drag of the body is determined either from a longitudinal accelerometer within the body, using the relationship

$$D = W \,.\, R_g$$

where W is the weight of the body (lb) a constant

R_g is the longitudinal accelerometer reading (g units),

or from the longitudinal deceleration of the body obtained by using other means such as double differentiation of position–time data, using the relationship

$$D = \left(\sin\theta - \frac{d^2s}{dt^2} \right) W$$

where θ is the attitude of body.

Thus for a complete determination of the problem, we need to know :

(*a*) the calibration of the atmosphere, i.e., p', T and the wind speed and direction at height,

(*b*) the trajectory of the body,

(*c*) if telemetering is to be used, the reading R_g of a longitudinal accelerometer in the body.

We now consider the accuracy of determination of R_g, V_a, p' and T, which are the basic quantities in the accuracy of the experiment.

3. *Accuracy of Measurements.*—3.1. *Velocity.*—We have two independent methods of determining V_s = true velocity in space. From the radar tracking of the trajectory we have

$$V_s = \frac{ds}{dt},$$

where s = distance along the trajectory, and from the telemetered longitudinal accelerometer reading we have

$$V_s = g\int_0^t (\sin\theta - R_g)\,dt + V_{s0},$$

where V_{s0} is the launching velocity.

Now the SCR.584 radar used in these experiments has automatic following in azimuth and elevation, and manual following in range. In azimuth and elevation, the radar follows from an error signal, *i.e.*, tracking correction demands are made on the following mechanism only when the tracking is in error by a certain minimum amount. Thus the radar hunts about the true position of the body. The magnitude of this minimum error is unknown, but is sufficient to show up in a plot of the recorded azimuth and elevation. Scatter in the range plot is due to the finite width and variations in quality of the echo. Hence the practice was to plot azimuth, elevation and range, draw smooth curves, and read off at 4-second intervals, using these smoothed values to compute the trajectory.

If R is the slant range (ft)

E is the angle of elevation (deg)

A is the azimuth angle (deg)

as given by radar, then in a typical case the following values apply.

	R	E	A
Scale resolution—from film record	20 ft	01′	01′
Resolution—from smoothed plot	50 ft	20′	12′
Typical absolute values	30,000 ft	0° to 70°	10° change

Now V_s is computed from triangulation of the trajectory at 4-second intervals,

$$\text{i.e., } V_s = \frac{\delta s}{\delta t} = \frac{1}{\delta t}\left[\left(\frac{R\,\delta A}{\sec E}\right)^2 + (\delta R)^2 + (R\,\delta E)^2\right]^{1/2}$$

The resultant velocity-time curve has the points scattered about the local smooth curve by about $\pm$ 5 per cent in a typical case. It is thus fairly clear that a second differentiation, to give acceleration, yields an answer of low accuracy, and, what is more important, one that masks the short time changes in drag in which we are interested.

Considering now the determination of V_s by integration from the longitudinal accelerometer reading, we have

$$\theta = \gamma - \varepsilon$$

where γ is the flight path angle

$$= \sin^{-1}\left[\frac{\delta(R \sin E)}{\delta s}\right]$$

ε is the correction due to wind

$$= \frac{v_w'}{V_s} \sin \gamma \text{ approximately}$$

v_w' is the component of headwind along body track.

In a typical case γ varies from 20 deg to 80 deg over the interesting part of a drop, and the computed values plot smoothly to about $\pm \frac{1}{4}$ deg. ε is small (usually not greater than 5 deg) and determinable to better than $\pm \frac{1}{2}$ deg. Assuming then in the worst case that the uncertainty in θ is $\pm \frac{1}{2}$ deg, we have absolute uncertainties in sin θ as shown in the following table.

Table Showing Significant Quantities in a Typical Drop
(Body Carrying 6·1 per cent Wings of 40-deg Sweep)

Mach number	0·38	0·6	0·8	0·9	1·0	1·1	1·2	1·27
Time from release (secs)	0	14	22	26	30	35	41	48 Splash
θ (deg)	0	49·3	60·2	64·0	67·3	71·2	75·1	78·8
sin θ	0	0·755	0·866	0·899	0·921	0·946	0·966	0·982
R_g	0·003	0·009	0·022	0·041	0·107	0·190	0·308	0·520
V_s (ft/sec)	370	605	815	925	1030	1160	1295	1420
(sin $\theta - R_g$)	−0·003	0·746	0·844	0·858	0·814	0·756	0·658	0·462
Δ(sin θ), $\delta\theta = \frac{1}{2}$ deg	0·009	0·005	0·004	0·004	0·003	0·003	0·002	0·002
$\Delta(R_g)$, 1 per cent full scale	0·006	0·006	0·006	0·006	0·006	0·006	0·006	0·006
Δ(sin $\theta - R_g$)	0·015	0·011	0·010	0·010	0·009	0·009	0·008	0·008
percentage error in V_s	—	1·3	1·3	1·3	1·3	1·3	1·3	1·3

Thus after about the first 10 seconds of the drop, the contribution from the uncertainty in R_g becomes the more significant, and leads to an uncertainty in V_s of the order, in this case, of 1·3 per cent. Note that in this example, we have assumed an accelerometer with a maximum reading of 0·6g, while the actual reading at splash is 0·52g, *i.e.*, we have assumed the drag of the body and the maximum accelerometer reading can be estimated with such confidence that a safety margin of about 15 per cent is sufficient. This, of course, is not always possible, and a greater margin is necessary to cover the uncertainties of estimation, with consequent loss of accuracy. On the other hand this body did not reach its terminal velocity; had it done so R_g would have risen to unity, with no loss of accuracy as far as drag measurement is concerned (provided the accelerometer is no worse matched to the maximum reading than is this example) but with some loss in the accuracy of determination of V_s (since (sin $\theta - R_g$) now approaches zero). It is not possible to consider the perfectly general problem arising here; we merely draw attention to the necessity for considering each case on its merits, bearing in mind the estimated drag characteristics of the model, its weight and the dropping height, and hence the speed and deceleration it is likely to have throughout its fall. Bearing in mind the Mach number range of interest it will usually be found desirable to use at least two accelerometers of different ranges.

Again, it has been assumed that R_g is reliable to $\pm$ 1 per cent ; this is an idealised figure better than was ever achieved even after the concentrated development during the last twelve months of the work described above, a more realistic order being $\pm$ 2 per cent. To compete with the contribution from sin θ, an accuracy in R_g of better than $\pm \frac{1}{2}$ per cent is required.

The true air velocity V_a is given by

$$V_a = V_s + v_w' \cos \gamma.$$

While the second term may well be zero, if the drop is made either in still-air conditions or when the wind is blowing at right-angles to the line of drop, in a typical case it varies from a maximum of 15 per cent of V_a at release to 1 per cent at splash. Assuming v_w' is determinable to $\pm$ 10 ft/sec (*see* below) there is an uncertainty at release of 2·5 per cent ; when $M > 0{\cdot}8$, i.e., $\theta > 50$ deg, the uncertainty in V_a is not likely to be worse than about $\pm$ 0·5 per cent.

The overall picture then is that V_a can be determined for the interesting part of a drop, *i.e.*, above a Mach number of 0·8, with an accuracy of about $\pm$ 1·5 per cent.

3.2. *Atmospheric Calibration.*—It has been shown above how we need to know the magnitude and direction of the wind at height ; in addition a knowledge is required of the variation of p' and T with height.

Originally air temperatures at altimeter heights were measured by the parent aircraft during ascents and descents, not necessarily over the bombing range, the variation of p' was assumed standard, and meteorological office predictions of wind at height were adopted. Latterly these characteristics of the atmosphere above the bombing range at the time of release were determined by flying the parent aircraft on a series of set courses at right-angles to the bombing run, at 5000-ft intervals from the release height down to 5000-ft, and tracking the aircraft by radar.

Since trajectory calculations are linked to accelerometer readings through time, and drag and velocity computations are made at 1 second intervals throughout the drop, the problem is to determine the relative pressure p' at a number of tape-measure heights, determined from

$$h_t = R \sin E + \text{(correction due to height of radar above sea-level)}.$$

The tie-up between h_t for the body trajectory and h_t for the aircraft during the calibrating runs can be done to $\pm$ 100 ft. Using the aircraft altimeter to measure the local pressure height h_p, an uncertainty of about $\pm$ 100 ft is introduced through inability to fly accurately at constant height, through errors in the altimeter calibration, and through errors in the determination of aircraft altimeter error due to venting. There is thus an uncertainty when comparing h_t and h_p of say 200 ft which, at the mean rate of change of p' between sea-level and 35,000 ft of 0·025 per 1000 ft, is an uncertainty in p' of about $\pm$ 0·005. In a typical drop $M = 0{\cdot}8$ at about 30,000ft when $p' = 0{\cdot}3$. Assuming a mean value of p' at 0·65, then this uncertainty is about $\frac{3}{4}$ per cent.

The rate of change of temperature with height is nearly 2 deg C per 1000 ft, and the rate of change of a, the velocity of sound, is nearly 2 ft/sec per 1 deg C. As before, we can effect the tie-up between the height of the body and the height of the aircraft during calibration runs to $\pm$ 100 ft, which corresponds to $\pm$ 0·2 deg C, and we can measure the air temperature to better than $\pm$ 1 deg C. The uncertainty in temperature is then about $\pm$ 1 deg C corresponding to an uncertainty in a of about 2 ft/sec or 0·2 per cent.

Attempts to improve accuracy by measuring the wind at height were inconclusive. Since only the component along the body trajectory is required, the first technique was to fly courses at right-angles to the body track, and to determine the wind component from the angle between the course and track of the aircraft. Various compass troubles and the lack of a suitable compass installation in the aircraft being used for this work, led to considerable scatter in the results,

which in consequence failed to provide, in the 3 cases in which this method was used, a reasonable basis for comparison between measurement and prediction. For the last body released the calibrating aircraft was flown along the track of the body, the wind component being determined from a comparison of aircraft course speed and radar track speed. In this instance the wind component was small—less than 30 ft/sec—and agreement between measurement and prediction to better than 10 ft/sec was obtained.

3.3. *Error in C_D.*—We have

$$\frac{\Delta C_D}{C_D} = \frac{\Delta R_g}{R_g} + \frac{\Delta p'}{p'} + 2\frac{\Delta a}{a} + 2\frac{\Delta V_a}{V_a}.$$

In the typical case so far considered, this gives the following results.

M	0·8	0·9	1·0	1·1	1·2	1·27
$\frac{\Delta R_g}{R_g}$, 1%	0·27	0·15	0·056	0·032	0·020	0·012
$\frac{\Delta p'}{p'}$	0·009	0·009	0·009	0·008	0·008	0·007
$2\frac{\Delta a}{a}$	0·005	0·004	0·004	0·003	0·003	0·003
$2\frac{\Delta V_a}{V_a}$	0·026	0·026	0·026	0·026	0·026	0·026
$\frac{\Delta C_D}{C_D}$	0·31	0·19	0·10	0·07	0·06	0·05
$\frac{\Delta R_g}{R_g}$, ½%	0·14	0·075	0·028	0·016	0·010	0·006
$2\frac{\Delta V_a}{V_a}$	0·021	0·020	0·020	0·019	0·018	0·017
$\frac{\Delta C_D}{C_D}$	0·18	0·11	0·06	0·05	0·04	0·03

The effect of improving the accuracy of R_g to ½ per cent of full-scale reading is shown ; the accuracy of the answer is approximately doubled.

4. *Discussion.*—It is clear from the previous discussion that the accuracy of this experiment depends primarily on the reliability of the telemetering equipment. As shown by the table in section 3.3, an accuracy of 1 per cent in the telemetering equipment does not in general give an answer of acceptable accuracy in the transonic region, where this experiment was intended to give its most useful answers. By combining telemetering equipment of a reliability of at least $\pm$ ½ per cent with a number of accelerometers of different full-scale ranges, and exercising considerable care in the determination of the relevant atmospheric data, useful answers should be possible, *i.e.*, drag differences between models of the order of 3 per cent of the total drag should be detectable with confidence. The method would then be comparable with wind-tunnel techniques.

REFERENCES

No.	Author	Title, etc.
1	R. McKinnon Wood	A suggested experiment to determine the drag of aerofoils at Mach numbers around unity. A.R.C. 7077. October, 1943. (Unpublished.)
2	The Staff of Supersonic Division, Flight Section.	Flight tests at transonic speeds on freely falling models. Part I : Models with 2-channel telemetering. R.A.E. Report Aero. 2180. S.D.16. A.R.C. 10,626. January, 1947. (Unpublished.)
3	The Staff of Supersonic Division, Flight Section.	Flight tests at transonic speeds on freely falling models. Part II : Tests on two further models. R.A.E. Report Aero. 2239. S.D. 25. A.R.C. 11,364. December, 1947. (Unpublished.)
4	Staff of Aero. Supersonics Flight Group	Flight tests at transonic speeds on freely falling models. Part III : Tests on rectangular wings of RAE 101 section. R.A.E. Report Aero. 2345. A.R.C. 13,584. July, 1950. (Unpublished.)
5	Staff of Aero. Supersonics Flight Group	Flight tests at transonic speeds on freely falling models. Part IV : Tests on untapered 40-deg swept-back wings of RAE 101 section. R.A.E. Report Aero. 2371. A.R.C. 13,596. May, 1950. (Unpublished.)
6	W. G. Molyneux and E. W. Chapple ..	Flutter experiments with freely falling models at high subsonic speeds. R.A.E. Report Structures 67. A.R.C. 13,722. May, 1950. (Unpublished.)
7	F. Smith	Note on use of flight models for investigation of flutter. R.A.E. Tech. Note Structures 11. A.R.C. 11,404. March, 1948. (Unpublished.)
8	W. L. Walters	Development and flight trials of a multi-channel telemetering system employing optical switching, for use in pressure-plotting experiments. R.A.E. Report Aero. 2405. October, 1950. (Unpublished.)
9	The Staff of Supersonic Division, Flight Section.	Flight trials of a rocket propelled transonic research model : The R.A.E.–Vickers rocket model. R. & M. 2835. March, 1950.
10	F. Smith and A. W. Thom	Note on the use of a longitudinal accelerometer for measuring aircraft drag in flight in the dive. R.A.E. Tech. Note Aero. 1649. June, 1945. (Unpublished.)
11	T. von Kármán	The similarity law of transonic flow. *J. Math. Phys.*, Vol. XXVI, No. 3, pp. 182 to 192. October, 1947.
12	S. M. Harmon	Theoretical supersonic wave drag of untapered swept-back and rectangular wings at zero lift. N.A.C.A. Tech. Note 1449. October, 1947.
13	W. E. Moeckel	Approximate method for predicting form and location of detached shock-waves ahead of plane or axially symmetric bodies. N.A.C.A. Tech. Note 1921. July, 1949.

TABLE 1

Model Data—Drag Measurements

	Units	Group I	Group II	Group III
Body				
Overall length	feet	13·42	14	14
Maximum diameter	inches	8	8	8
Frontal area	square feet	0·349	0·349	0·349
Nose curvature radius	body diameters	3	3	3
Fin				
Exposed semi-span	inches	10·5	9	9
Chord (root)	inches	9	18	18
Chord (tip)	inches	9	10·5	10·5
Number per model		4	4	4
Net area	square feet	2·625	3·56	3·56
Thickness	inches	0·625	0·160	0·160
Net frontal area	square feet	0·182	0·040	0·040
Wing				
Span	feet	6	6	6
Chord (right-angles to (leading edge)	inches	20	20	20
Chord (in direction of free stream)	inches	20	20	26·1
Gross area	square feet	10	10	10·34
Net area	square feet	8·89	8·89	8·89
Section		Symmetrical biconvex	RAE 101	RAE 101
Gross aspect ratio		3·6	3·6	2·18
Net aspect ratio		3·2	3·2	1·88
Taper ratio		1·0	1·0	1·0
Leading-edge sweepback	degrees	0	0	40

Group I Models

	Model 1	Model 2	Model 3	Model 4	Model 5
Wing thickness/chord ratio	0·05	0·08	0·12	No wing (Free fall)	No wing (Free fall dummy)
Net wing frontal area (sq ft)	0·444	0·711	1·067	—	—
Gross frontal area of model (sq ft)	0·975	1·242	1·598	0·531	0·531
Model weight (lb)	1630	1716	1717	1670	378

TABLE 1—*continued*

Group II Models

	Model 6	Model 7	Model 9	Model 10	Model 10	Model 11	Model 12
Wing thickness/chord ratio	0·05	0·08	0·12	No wing (free fall)	No wing (free fall)	No wing (ground-launched)	No wing (ground-launched)
Net wing frontal area (sq ft)	0·444	0·711	1·067	—	—	—	—
Gross frontal area of model (sq ft)	0·833	1·100	1·456	0·389	0·389	0·316	0·316
Model weight (lb)	1480	1382	1371	1354	1322	90·6	100·8

Group III Models

	Model 13	Model 14	Model 15
Wing thickness/chord ratio (free-stream direction)	0·038	0·061	0·092
Wing thickness/chord ratio (right-angles to leading edge)	0·05	0·08	0·12
Wing net frontal area (sq ft)	0·340	0·544	0·817
Gross frontal area of model (sq ft)	0·729	0·933	1·206
Model Weight (lb)	1699	1848	1385

Note: Results from models 9, 10, 11 and 12 were also used in the analysis of the results for models 13, 14 and 15.

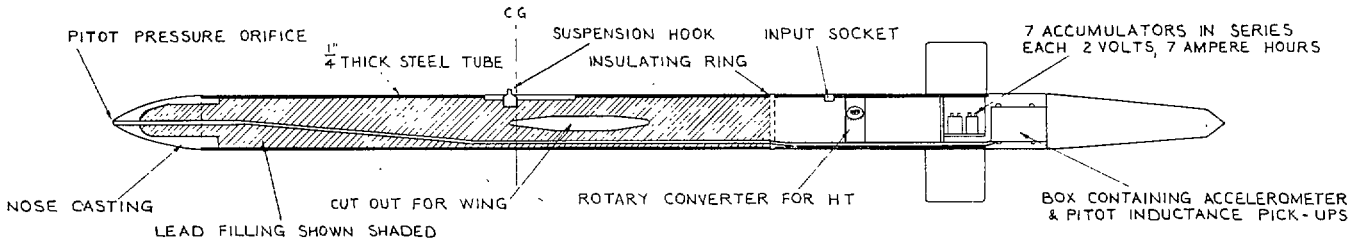

CUT AWAY VIEW OF TYPE 'A' BODY.

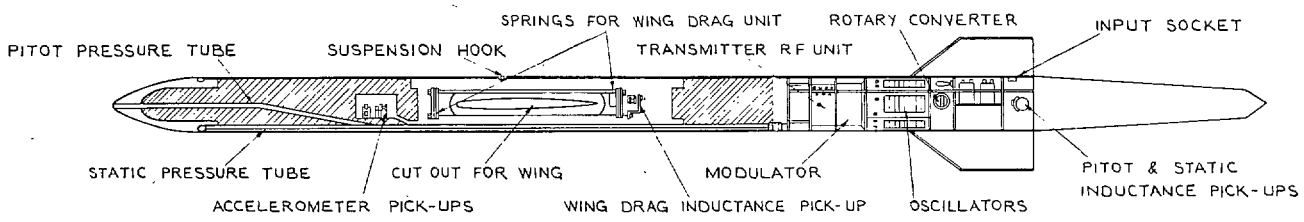

CUT AWAY VIEW OF TYPE 'B' BODY.

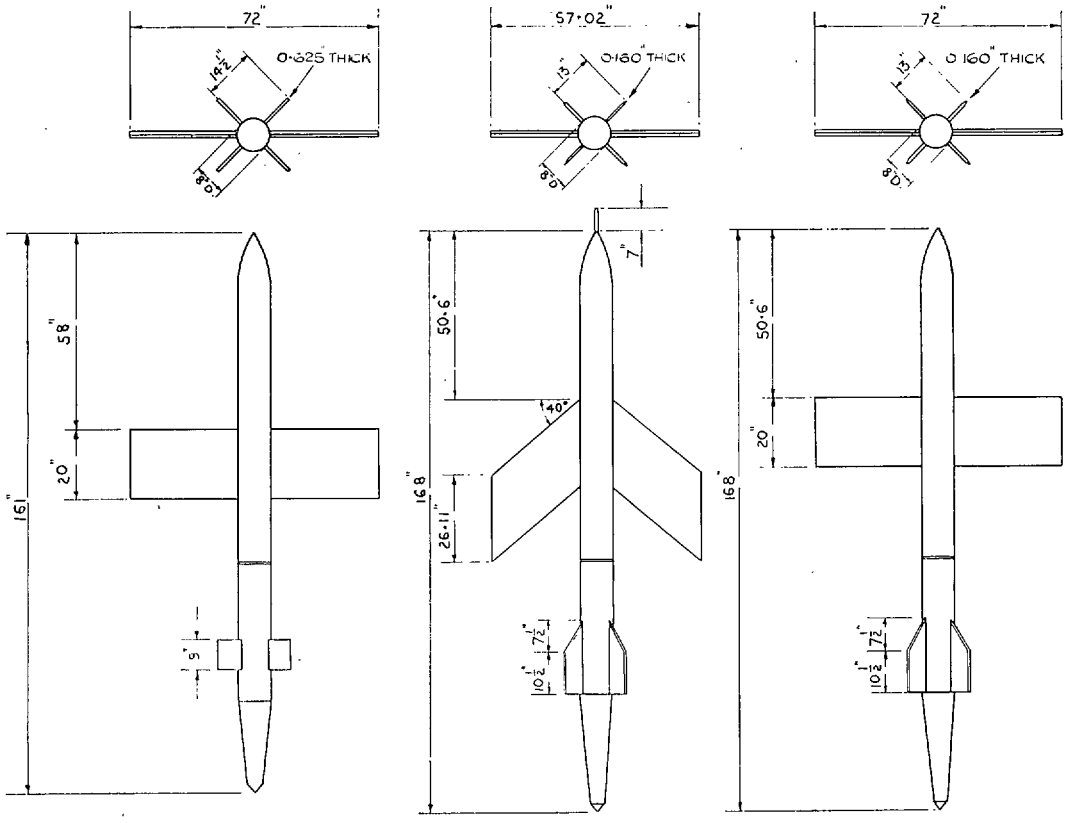

TYPE 'A' BODY CARRYING RECTANGULAR WINGS. GROUP I

TYPE 'B' BODY CARRYING SWEPT BACK WINGS GROUP III

TYPE 'B' BODY CARRYING RECTANGULAR WINGS. GROUP II

FIG. 1. General arrangement of models.

FIG. 2. Installation of winged model on *Mosquito*.

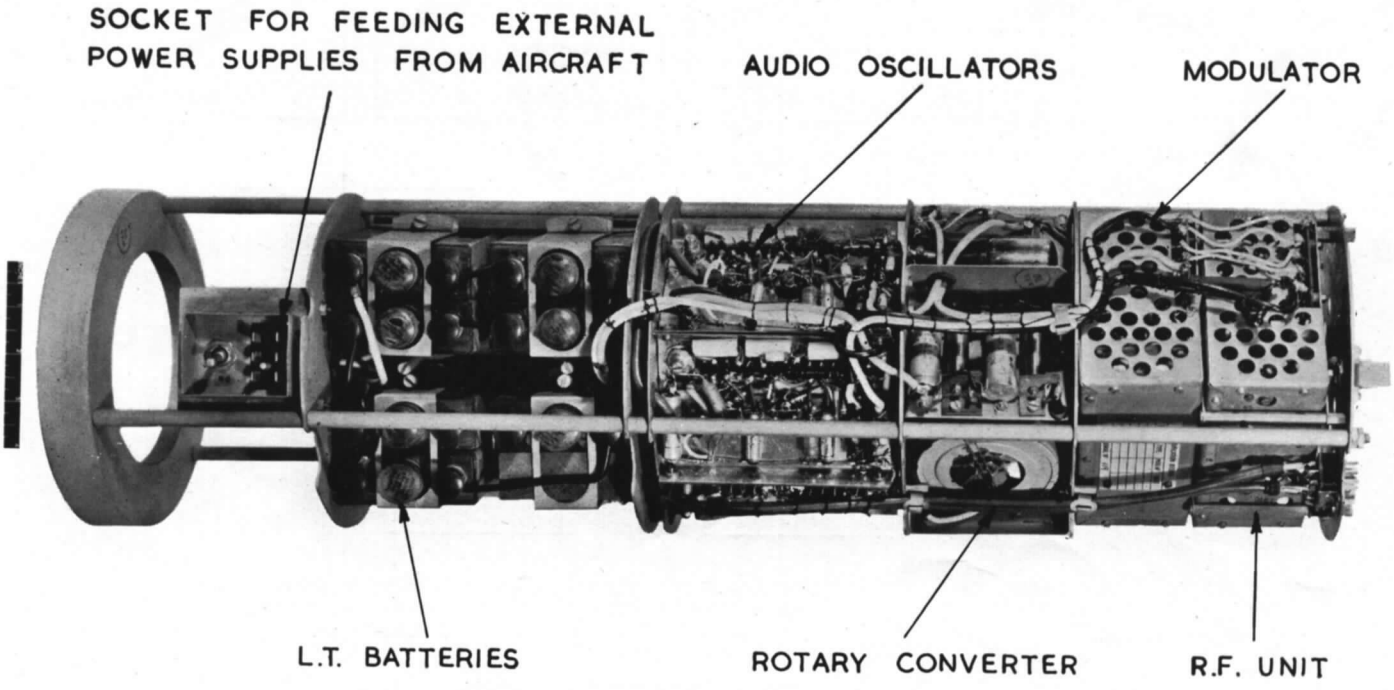

FIG. 3. Six-channel telemetering transmitter used in Type B bodies.

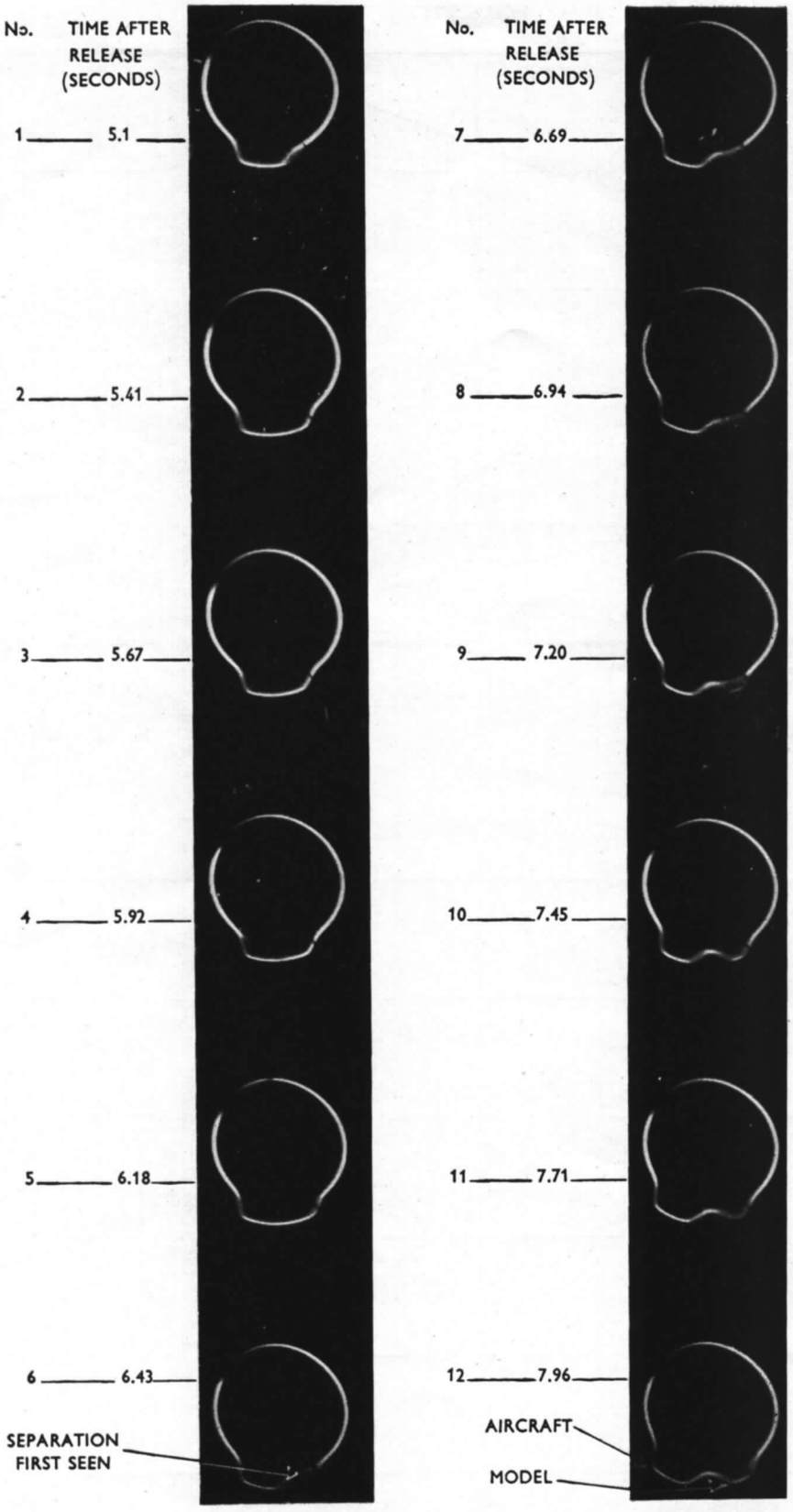

FIG. 4. Separation of model from aircraft as seen on radar range oscilloscope.

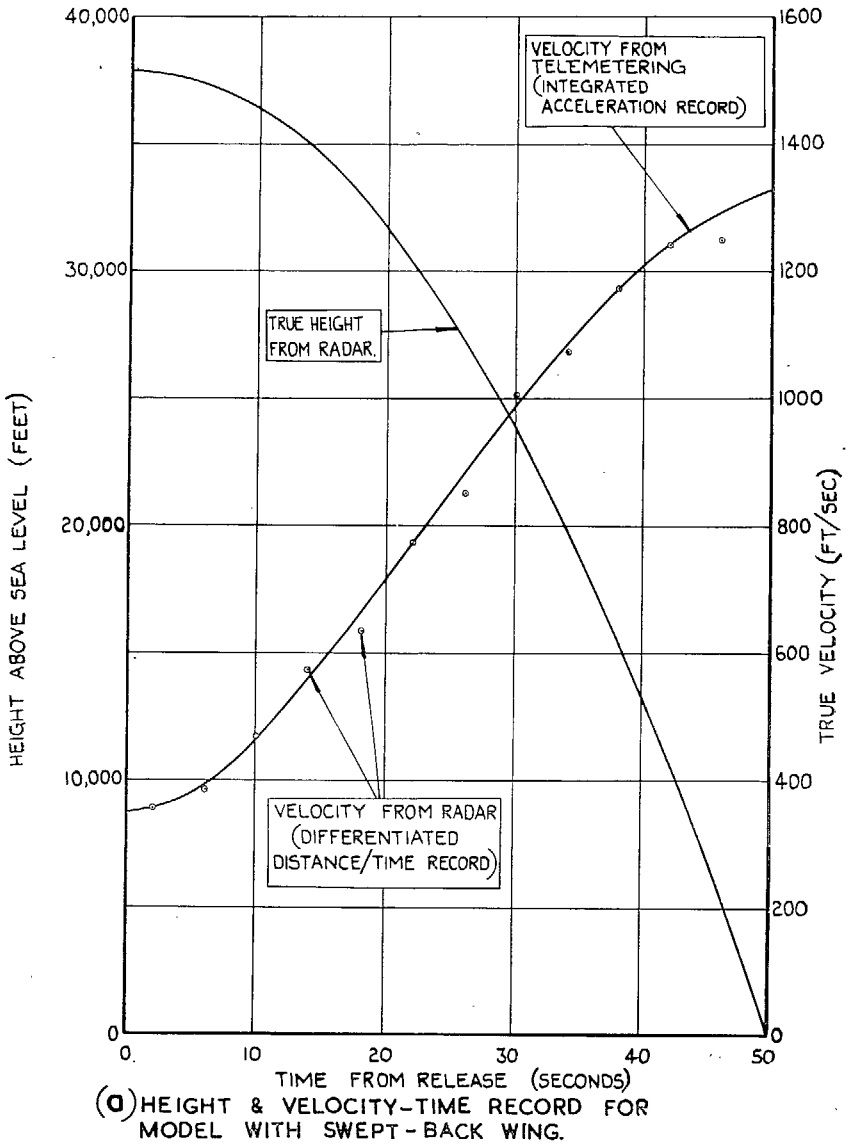

(a) HEIGHT & VELOCITY–TIME RECORD FOR MODEL WITH SWEPT-BACK WING.

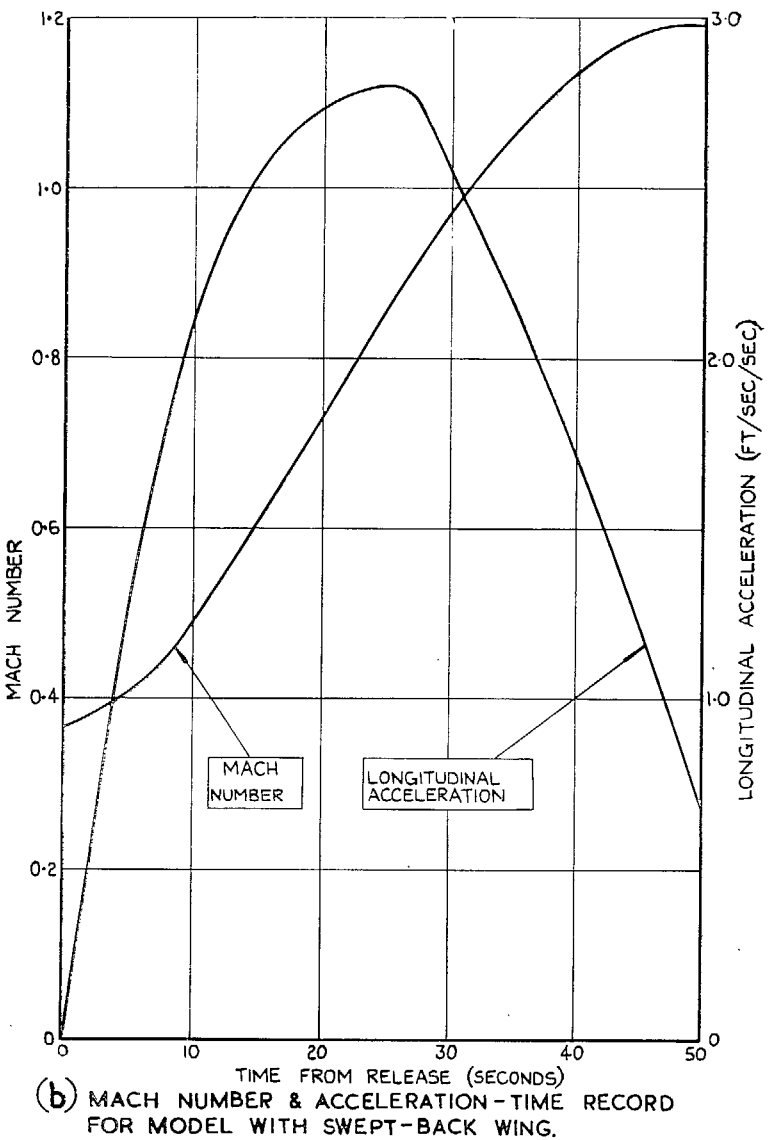

(b) MACH NUMBER & ACCELERATION–TIME RECORD FOR MODEL WITH SWEPT-BACK WING.

FIGS. 5a and 5b. Trajectory characteristics of typical model.

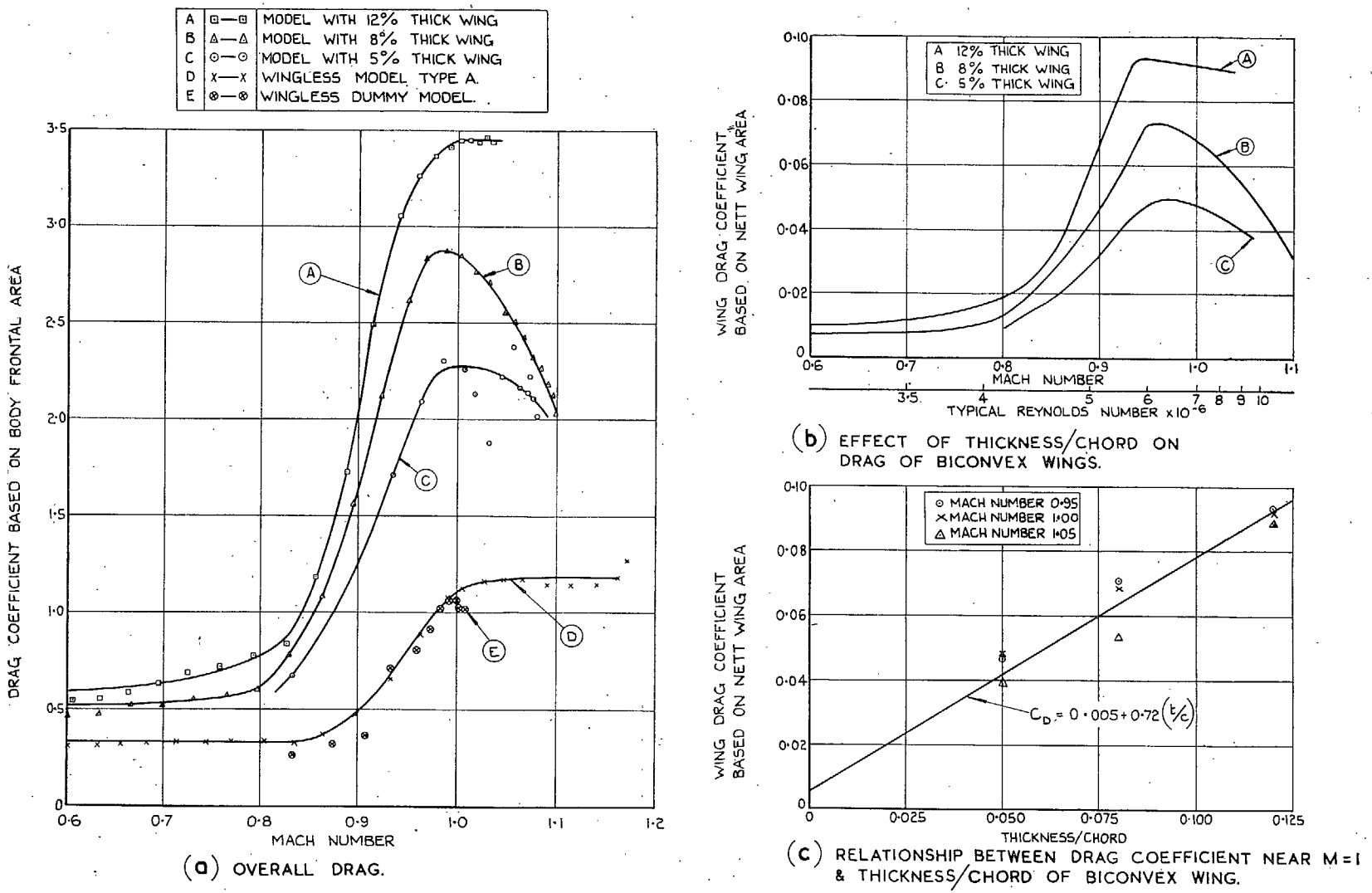

FIGS. 6a, 6b and 6c. Drag characteristics of Group I models.

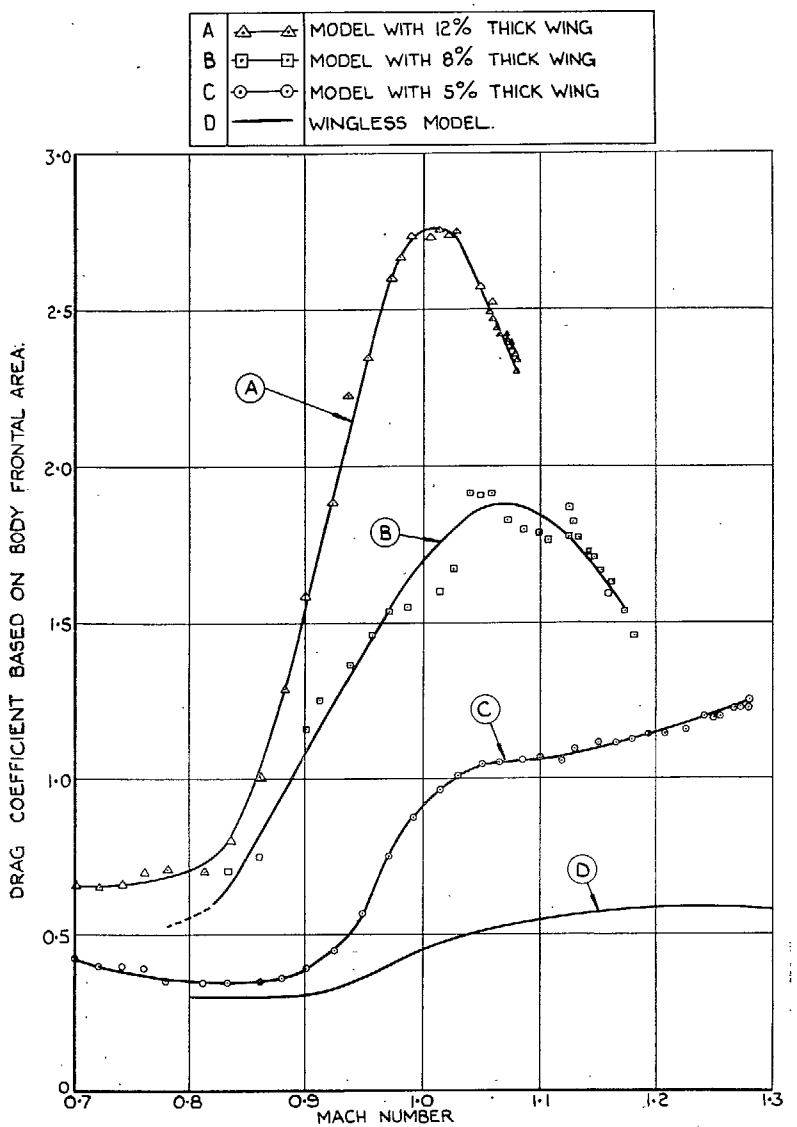

(a) OVERALL DRAG.

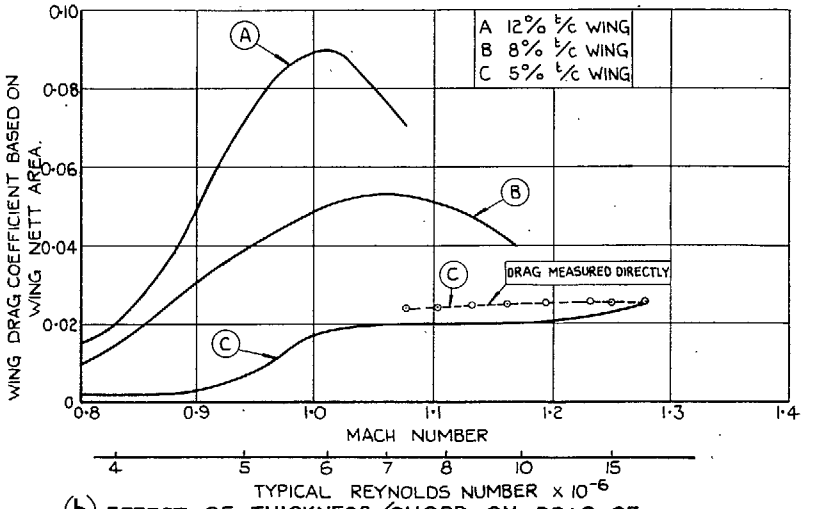

(b) EFFECT OF THICKNESS/CHORD ON DRAG OF RECTANGULAR WINGS OF R.A.E. 101 SECTION.

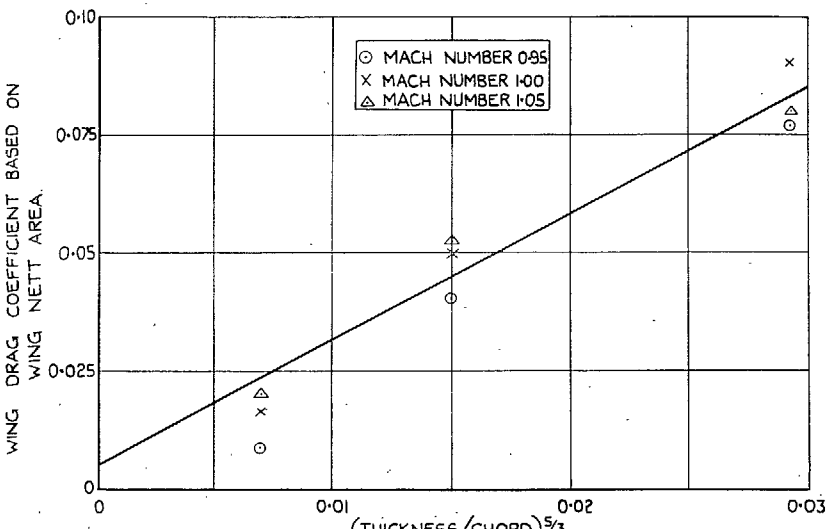

(c) RELATIONSHIP BETWEEN DRAG COEFFICIENT NEAR M = 1 & (THICKNESS/CHORD)$^{5/3}$

FIGS. 7a, 7b and 7c. Drag characteristics of Group II models.

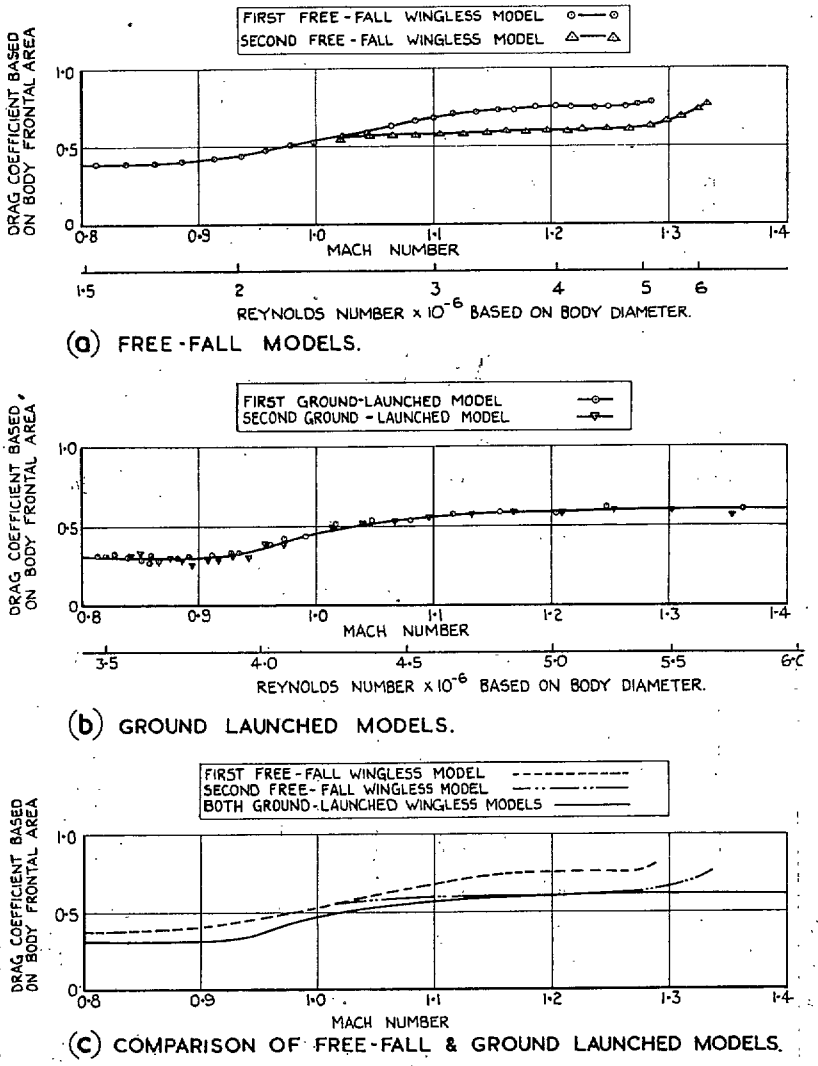

FIGS. 8a, 8b and 8c. Free-fall and ground-launched Type B models without wings.

CURVE	NETT ASPECT RATIO	Λ°	THICKNESS/CHORD	
			AT RT. ANGLES TO L.E.	IN FREE STREAM DIRECTION
A	1·88	40	12%	9·19%
B	1·88	40	8%	6·13%
C	1·88	40	5%	3·83%
D	WINGLESS MODEL			

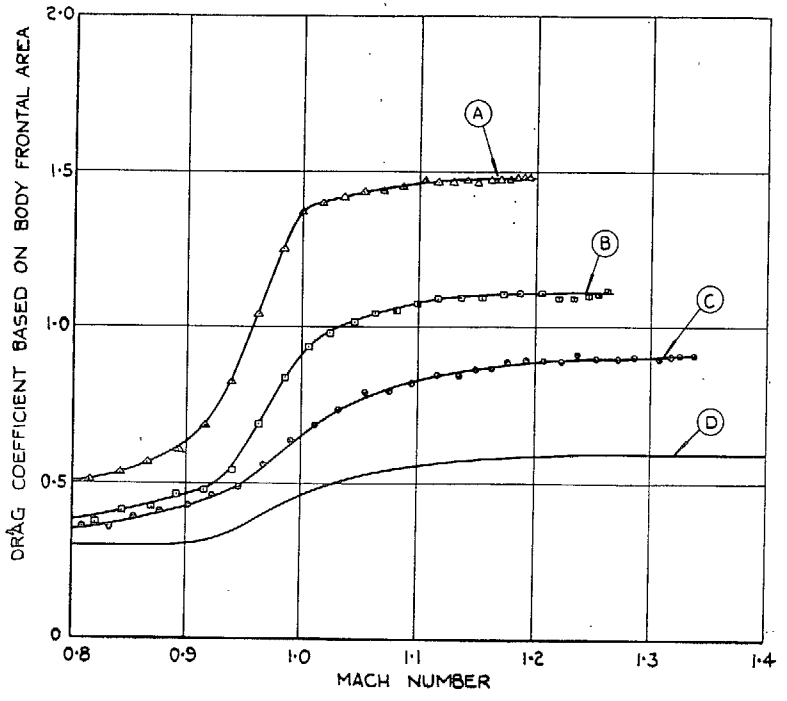

(a) OVERALL DRAG.

CURVE	NETT ASPECT RATIO	Λ°	THICKNESS/CHORD	
			AT RT. ANGLES TO L.E.	IN FREE STREAM DIRECTION
A	1·88	40	12%	9·19%
B	1·88	40	8%	6·13%
C	1·88	40	5%	3·83%

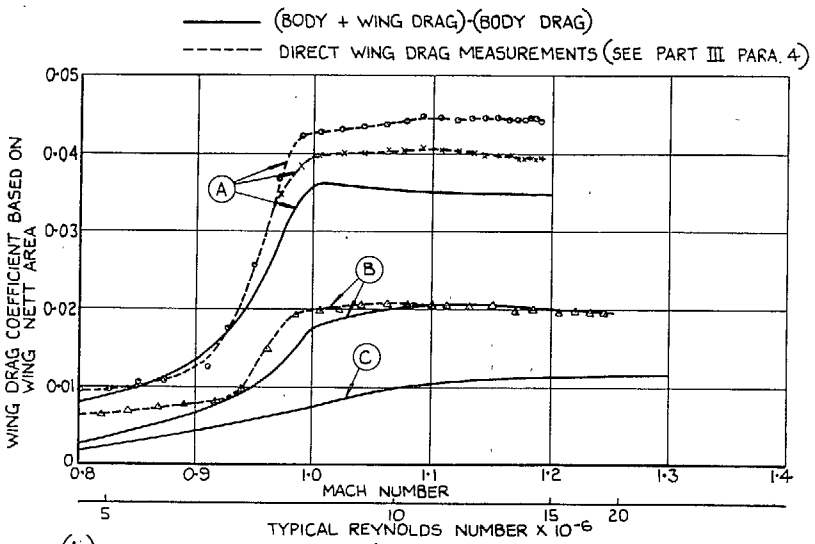

(b) EFFECT OF THICKNESS/CHORD ON DRAG OF SWEPT-BACK WINGS OF R.A.E. 101 SECTION.

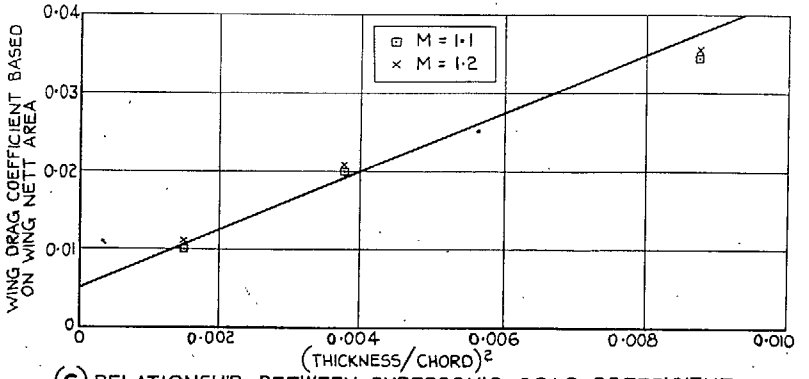

(c) RELATIONSHIP BETWEEN SUPERSONIC DRAG COEFFICIENT & (THICKNESS/CHORD)².

FIGS. 9a, 9b and 9c. Drag characteristics of Group III models.

CURVE	NETT ASPECT RATIO	$\Lambda°$	THICKNESS/CHORD AT RT ANGLES TO L.E.	THICKNESS/CHORD IN FREE STREAM DIRECTION
A	3·2	0	12%	12%
B	3·2	0	8%	8%
C	3·2	0	5%	5%
D	1·88	40	12%	9·19%
E	1·88	40	8%	6·13%
F	1·88	40	5%	3·83%

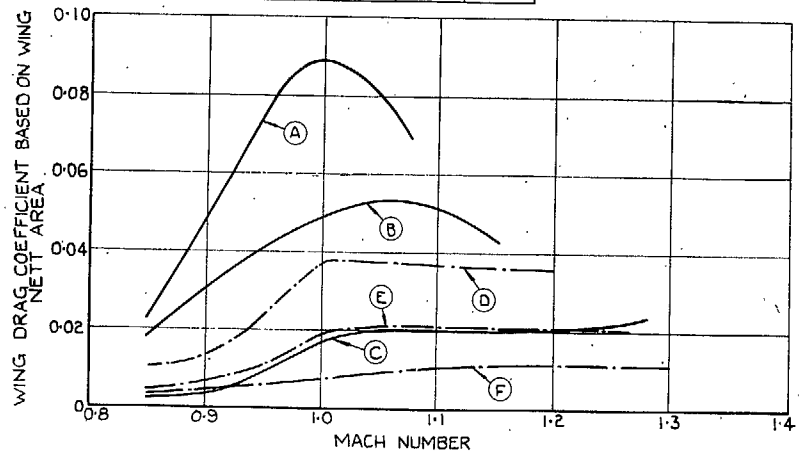

FIG. 10. Comparison of swept and unswept wings of varying thickness ratios.

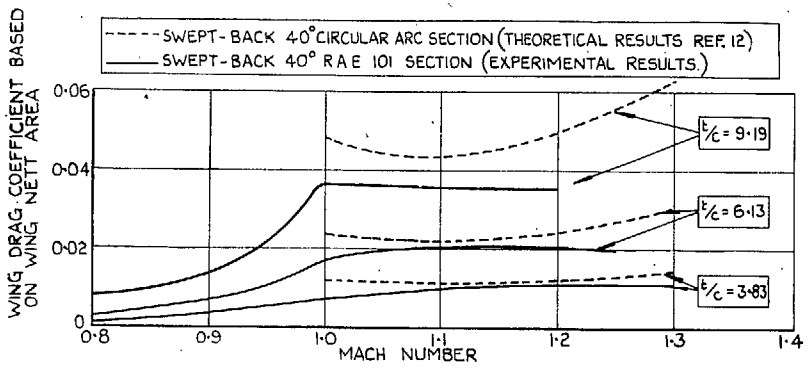

FIG. 11. Comparison of experiment and theory for swept-back wings.

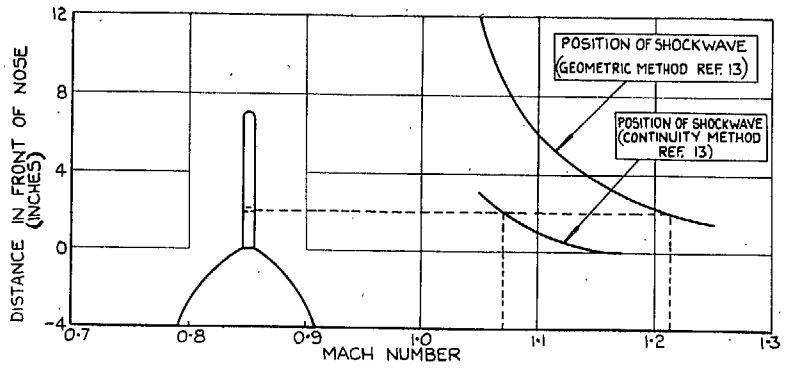

FIG. 12. Position of shock-wave in front of nose.

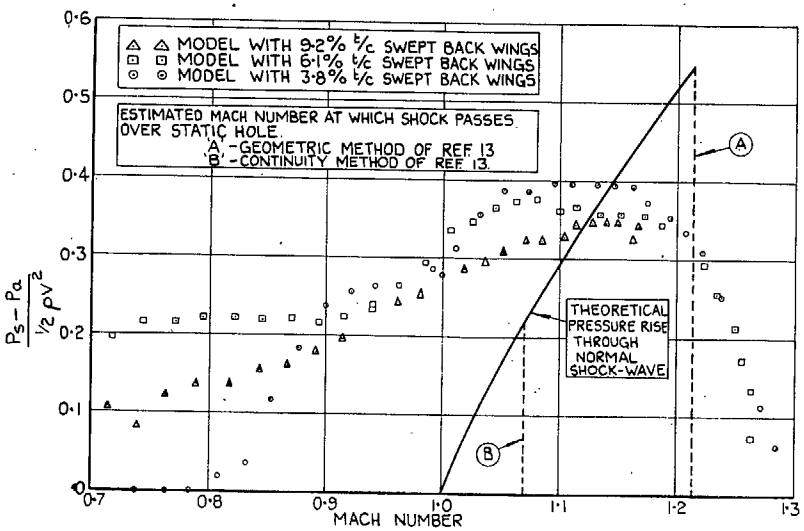

FIG. 13. Position error on static head.

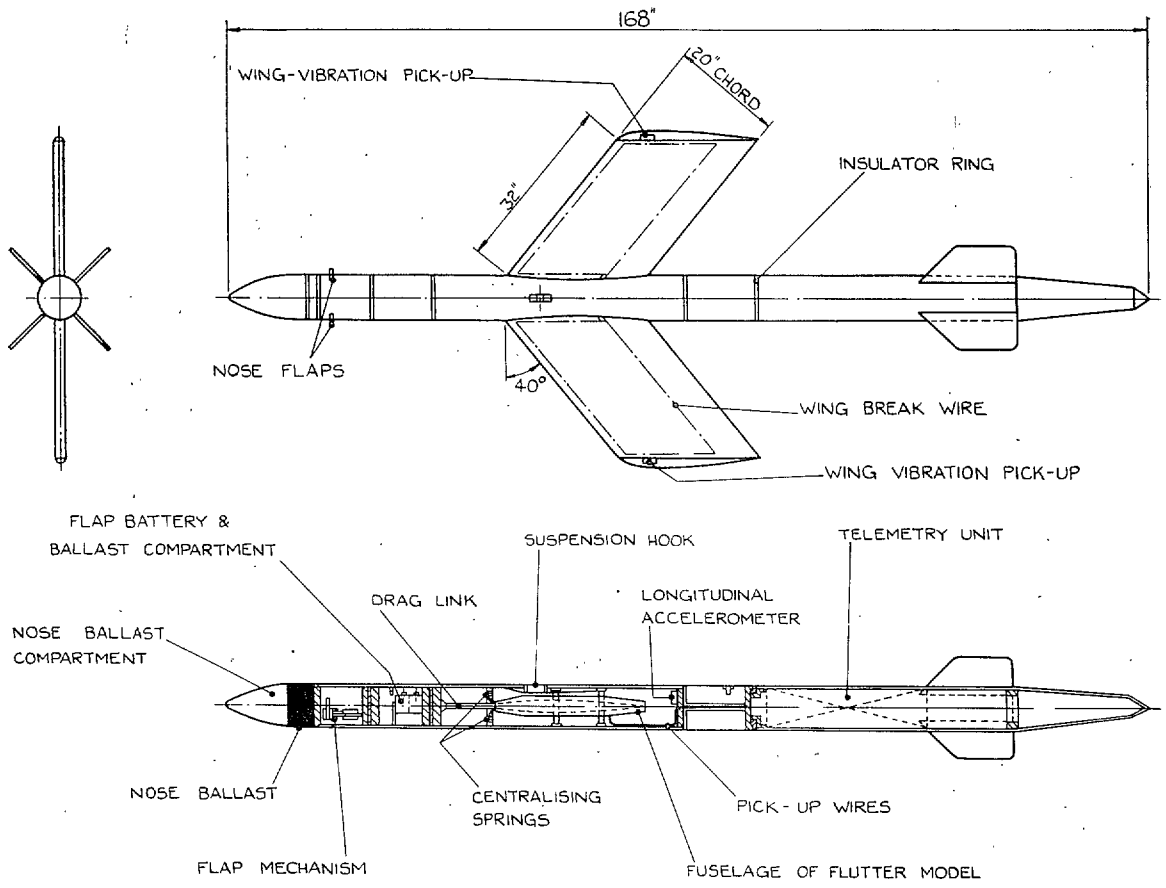

FIG. 14. General arrangement of flutter model. (40-deg swept-back wing with Type B2 body.)

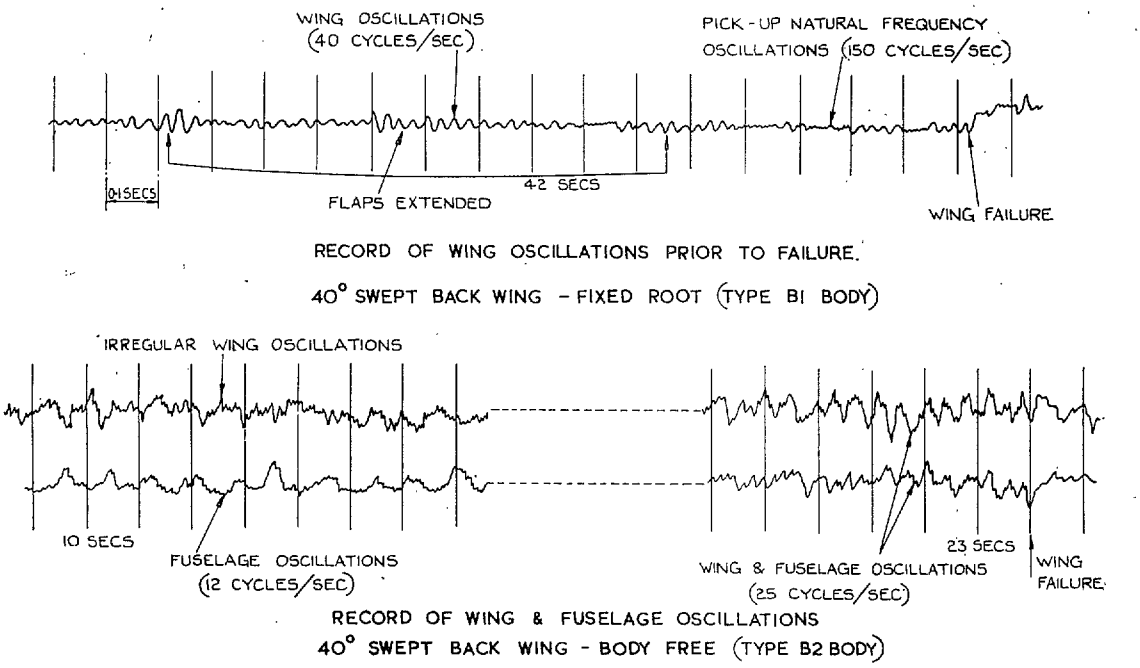

FIG. 15. Records of wing flutter.

J4325 Wt.18/9296 K7 6/55 D&Co. 34/263

PRINTED IN GREAT BRITAIN

Publications of the Aeronautical Research Council

ANNUAL TECHNICAL REPORTS OF THE AERONAUTICAL RESEARCH COUNCIL (BOUND VOLUMES)

1936 Vol. I. Aerodynamics General, Performance, Airscrews, Flutter and Spinning. 40*s.* (41*s.* 1*d*).

Vol. II. Stability and Control, Structures, Seaplanes, Engines, etc. 50*s.* (51*s.* 1*d.*)

1937 Vol. I. Aerodynamics General, Performance, Airscrews, Flutter and Spinning. 40*s.* (41*s.* 1*d.*)

Vol. II. Stability and Control, Structures, Seaplanes, Engines, etc. 60*s.* (61*s.* 1*d.*)

1938 Vol. I. Aerodynamics General, Performance, Airscrews. 50*s.* (51*s.* 1*d.*)

Vol. II. Stability and Control, Flutter, Structures, Seaplanes, Wind Tunnels, Materials. 30*s.* (31*s.* 1*d.*)

1939 Vol. I. Aerodynamics General, Performance, Airscrews, Engines. 50*s.* (51*s.* 1*d.*)

Vol. II. Stability and Control, Flutter and Vibration, Instruments, Structures, Seaplanes, etc. 63*s.* (64*s.* 2*d.*)

1940 Aero and Hydrodynamics, Aerofoils, Airscrews, Engines, Flutter, Icing, Stability and Control, Structures, and a miscellaneous section. 50*s.* (51*s.* 1*d.*)

1941 Aero and Hydrodynamics, Aerofoils, Airscrews, Engines, Flutter, Stability and Control, Structures. 63*s.* (64*s.* 2*d.*)

1942 Vol. I. Aero and Hydrodynamics, Aerofoils, Airscrews, Engines. 75*s.* (76*s.* 3*d.*)

Vol. II. Noise, Parachutes, Stability and Control, Structures, Vibration, Wind Tunnels. 47*s.* 6*d.* (48*s.* 7*d.*)

1943 Vol. I. Aerodynamics, Aerofoils, Airscrews, 80*s.* (81*s.* 4*d.*)

Vol. II. Engines, Flutter, Materials, Parachutes, Performance, Stability and Control, Structures. 90*s.* (91*s.* 6*d.*)

1944 Vol. I. Aero and Hydrodynamics, Aerofoils, Aircraft, Airscrews, Controls. 84*s.* (85*s.* 8*d.*)

Vol. II. Flutter and Vibration, Materials, Miscellaneous, Navigation, Parachutes, Performance, Plates, and Panels, Stability, Structures, Test Equipment, Wind Tunnels. 84*s.* (85*s.* 8*d.*)

ANNUAL REPORTS OF THE AERONAUTICAL RESEARCH COUNCIL—

1933–34	1*s.* 6*d.* (1*s.* 8*d.*)	1937	2*s.* (2*s.* 2*d.*)
1934–35	1*s.* 6*d.* (1*s.* 8*d.*)	1938	1*s.* 6*d.* (1*s.* 8*d.*)
April 1, 1935 to Dec. 31, 1936.	4*s.* (4*s.* 4*d.*)	1939–48	3*s.* (3*s.* 2*d.*)

INDEX TO ALL REPORTS AND MEMORANDA PUBLISHED IN THE ANNUAL TECHNICAL REPORTS, AND SEPARATELY—

April, 1950 – – – – R. & M. No. 2600. 2*s.* 6*d.* (2*s.* 7½*d.*)

AUTHOR INDEX TO ALL REPORTS AND MEMORANDA OF THE AERONAUTICAL RESEARCH COUNCIL—

1909–1949 – – – – – R. & M. No. 2570. 15*s.* (15*s.* 3*d.*)

INDEXES TO THE TECHNICAL REPORTS OF THE AERONAUTICAL RESEARCH COUNCIL—

December 1, 1936 — June 30, 1939.	R. & M. No. 1850.	1*s.* 3*d.* (1*s.* 4½*d.*)
July 1, 1939 — June 30, 1945.	R. & M. No. 1950.	1*s.* (1*s.* 1½*d.*)
July 1, 1945 — June 30, 1946.	R. & M. No. 2050.	1*s.* (1*s.* 1½*d.*)
July 1, 1946 — December 31, 1946.	R. & M. No. 2150.	1*s.* 3*d.* (1*s.* 4½*d.*)
January 1, 1947 — June 30, 1947.	R. & M. No. 2250.	1*s.* 3*d.* (1*s.* 4½*d.*)
July, 1951 – – – –	R. & M. No. 2350.	1*s.* 9*d.* (1*s.* 10½*d.*)

Prices in brackets include postage.

Obtainable from

HER MAJESTY'S STATIONERY OFFICE

York House, Kingsway, London W.C.2 ; 423 Oxford Street, London W.1 (Post Orders : P.O. Box No. 569, London S.E.1) ; 13A Castle Street, Edinburgh 2 ; 39 King Street, Manchester 2 ; 2 Edmund Street, Birmingham 3 ; 109 St. Mary Street, Cardiff ; Tower Lane, Bristol 1 ; 80 Chichester Street, Belfast OR THROUGH ANY BOOKSELLER

S.O. Code No. 23-2902